Response to Referee #1

We thank the reviewer for taking the time to review this manuscript and provide valuable and constructive suggestions/comments. We have addressed all the points one-by-one raised by the reviewer (copied here and shown in black text) along with the corresponding reply from the authors (in blue text, page and line number in revised version).

1) P1—L1: the title contains a few acronyms and would be complicated if spelling out their full names. I would recommend a brief title, such as "Intercomparison of arctic XH_2O observations from three ground based FTIR networks and application for satellite validation".

The recommended title is brief and it is a very good suggestion. We are happy to have this new title, which is easier to understand for a broader community.

2) P1—L17: it is better to specify the time period here.

The time period for COCCON datasets is between March 6, 2017 and September 20, 2019. It is added according to referee's comment (P1-Line18).

3) P3—L92: "ESA" to "European Space Agency (ESA)". The full name of an acronym should be spelled out when it first appears.

We modified the text according to the referee's comment (P3-line 92).

4) P4—L99: "European Space Agency (ESA)" to "ESA", when the full name of an acronym is already mentioned before.

We modified the text according to the referee's comment (P4-line 100).

5) P5—L139, L140: spell out the full name of WACCM and ESSD.

The WACCM refers to Whole Atmosphere Community Climate Model and ESSD refers to Earth System Science Data.

We modified the text according to the referee's comment (P5-line 140 and 141).

6) P6—L174: does a similar airmass bias correction is applied to COCCON as used in TCCON? please elaborate a bit more or a reference here.

The airmass dependent correction is mainly resulting from existing imperfections of the spectroscopic line lists. TCCON data are corrected for systematic errors representing spurious diurnal variation and therefore, adjusted to in-situ/WMO trace gas units by using a large number of in-situ aircraft profiles (Wunch et al., 2011). A similar posteriori-dependent airmass bias correction is applied to COCCON in order to also link COCCON data to the WMO standard via TCCON (Frey et al., 2019)

7) P7—L198: the formula here defines the total mixing ratio of H2O (wet mixing ratio) rather than dry mixing ratio. In section 4.3, the map and radiosonde profiles are investigated. Are MAP H2O a priori profiles also a wet mixing ratio? If so, the use of "XH_2O" as the volume mixing ratio of H2O by integrating the a priori MAP profiles and radiosonde profiles in Figure 8 will confuse readers, since the XH_2O is defined as "dry-air mole fractions of water vapor" in the very beginning of this work.

The TCCON a priori profiles are treated as if it is a wet mole fraction (https://tccon-wiki.caltech.edu/Main/AuxilaryData). Integrated radiosonde XH_2O and MAP XH_2O in Figure 8 and Figure 9 are updated to dry-air mole fraction of H_2O.

$$X_{H_2O} = \frac{P_{H_2O}}{P - P_{H_2O}} = \frac{f_{H_2O}}{1 - f_{H_2O}}$$

f_{H_2O} is the mole fraction of H_2O in the air.

8) P8—L215: could you elaborate a bit more on this seasonal variation of XH_2O? or a reference here.

The following explanations have been added (P8-219).

Specific humidity shows a strong positive correlation with temperature (Issac and Wijngaarden, 2012). Meanwhile, the higher precipitation in summer intensifies the higher atmospheric water vapor concentration. The evaporation from the snow-covered continent and frozen water surface is still much less, limiting the transport of water vapor into the atmosphere. This effect lasts until spring due to the slow warming of the surface (Wypych et al., 2018).

Isaac, V., and van Wijngaarden, W. A. Surface Water Vapor Pressure and Temperature Trends in North America during 1948–2010. J. Climate, 25, 3599–3609, https://doi.org/10.1175/JCLI-D-11-00003.1, 2012.
Wypych, A., Bochenek, B. and Różycki, M.: Atmospheric Moisture Content over Europe and the Northern Atlantic. Atmosphere, 9, 18, https://doi.org/10.3390/atmos9010018, 2018.

9) P17—L358: MUSICA IASI might be not considered as "network". It is better to change to "…due to the choices for the calibration of XH_2O data product by either dataset."

We modified the text according to the referee's comment (P17-line 368).

10) P18—L366: it is better to keep the two subsections' names consistency. Change "Comparison between TROPOMI and COCCON" to "Comparison between COCCON and TROPOMI" or the other way around.

We modified the text according to the referee's comment (P18-line 374).

Response to Referee #2

We thank the reviewer for taking the time to review this manuscript and provide valuable and constructive suggestions/comments. We have addressed all the points one-by-one raised by the reviewer (copied here and shown in black text) along with the corresponding reply from the authors (in blue text).

1) Some readers are maybe interested in a bit more details about the COCCON-XH_2O retrieval itself, maybe this could be added very easy in section 2.2. What are the used microwindows, and linelist and if the XH_2O is calibrated against TCCON or Musica in Karlsruhe, how large are these calibration factors, and how are they calculated.

The COCCON H_2O is retrieved in the spectral window of 8353.4 – 8463.1 cm^{-1}. The updated HITRAN 2009 linelist with empirical corrections is used in the PROFFAST. A universal calibration factor of 0.83 is applied to XH_2O as a post correction in PROFFAST.

2) Summary of information for different products used in this study.

The table below has been added to the manuscript.

	COCCON	TCCON	MUSICA NDACC	MUSICA IASI	TROPOMI
Spectral window (cm^{-1})	8353.4 – 8463.1	4565.2 – 6469.6 (Wunch et al., 2015)	2658 – 3053	1190 – 1400	4200.8 – 4248.1 (Scheepmaker et al., 2016)
Spectroscopic modelling	HITRAN 2009	HITRAN 2009	HITRAN 2012 with modifications to consider speed-dependent Voigt line shapes (Barthlott et al., 2017)	HITRAN 2016, Voigt line shapes Water vapor continuum model: MT_CKD v2.5.2 (Delamere et al., 2010; Payne et al., 2011; Mlawer et al., 2012)	HITRAN 2016
A priori H_2O	NCEP/ NCAR[1]	NCEP/ NCAR	Globally mean WACCM[2] profile. No latitudinal and seasonal dependence	Latitudinal-and-seasonal dependent WACCM climatology	ECMWF[3]
Calibration factor	0.830	1.0183 (Wunch et al., 2015)	0.88	None	None
Number of degrees of freedom			2.8	4-5	

[1] National Centers for Environmental Prediction/National Center for Atmospheric Research

[2] Whole Atmosphere Community Climate Model

[3] European Centre for Medium-Range Weather Forecasts

Barthlott, S., Schneider, M., Hase, F., Blumenstock, T., Kiel, M., Dubravica, D., García, O. E., Sepúlveda, E., Mengistu Tsidu, G., Takele Kenea, S., Grutter, M., Plaza-Medina, E. F., Stremme, W., Strong, K., Weaver, D., Palm, M., Warneke, T., Notholt, J., Mahieu, E., Servais, C., Jones, N., Griffith, D. W. T., Smale, D., and Robinson, J.: Tropospheric water vapour isotopologue data (H216O, H218O, and HD16O) as obtained from NDACC/FTIR solar absorption spectra, Earth Syst. Sci. Data, 9, 15–29, https://doi.org/10.5194/essd-9-15-2017, 2017.

Delamere, J. S., Clough, S. A., Payne, V. H., Mlawer, E. J., Turner, D. D. and Gamache, R. R.: A far-infrared radiative closure study in the Arctic: application to water vapor. J. Geophys. Res. 115, D17106. doi:10.1029/2009JD012968, 2010.

Mlawer, E. J., Payne, V. H., Moncet, J.-L., Delamere, J. S., Alvarado, M. J. and Tobin, D. C.: Development and recent evaluation of the MT_CKD model of continuum absorption. Phil. Trans. R. Soc. A.3702520–2556 http://doi.org/10.1098/rsta.2011.0295, 2012.

Payne, V. H., Mlawer, E. J., Cady-Pereira, K. E. and Moncet, J.-L.: Water Vapor Continuum Absorption in the Microwave. Geoscience and Remote Sensing, IEEE Transactions on. 49. 2194 - 2208. 10.1109/TGRS.2010.2091416, 2011.

Scheepmaker, R. A., aan de Brugh, J., Hu, H., Borsdorff, T., Frankenberg, C., Risi, C., Hasekamp, O., Aben, I., and Landgraf, J.: HDO and H2O total column retrievals from TROPOMI shortwave infrared measurements, Atmos. Meas. Tech., 9, 3921–3937, https://doi.org/10.5194/amt-9-3921-2016, 2016.

Wunch, D., Toon, G. C., Sherlock, V., Deutscher, N. M., Liu,C., Feist, D. G., and Wennberg, P. O.: The Total CarbonColumn Observing Network's GGG2014 Data Version, Tech.rep., California Institute of Technology, Carbon Dioxide In-formation Analysis Center, Oak Ridge National Laboratory,Oak Ridge, Tennessee, USA, https://doi.org/10.14291/tccon.ggg2014.documentation.R0/1221662, 2015.

3) A rough statement on the precision of a single XH_2O COCCON measurement and its duration and how these two numbers compare to the TCCON and NDACC-MUSICA measurements.

The COCCON instrument records one spectrum in about 58 seconds. TCCON instrument records one forward-backward scan in 156.7 seconds, i.e. one measurement takes 78 seconds. An NDACC high resolution measurement used for the MUSICA retrieval takes about 8 minutes. The precision of total column MUSICA NDACC data is theoretically estimated to 1% (see Table 3 in Schneider et al., 2012).

4) Could you calculate the impact of the different aprioris theoretically and explain the 1% difference between the MUSICA IASI and MUSICA IASI (MAP)

There is no calibration factor applied to MUSICA IASI data. The MUSICA IASI data are obtained from HITRAN 2016 Voigt line shape parameters and the continuum model MT_CKD v2.5.2. This 5% bias is likely a bias in the MUSICA IASI data and it is in line with the uncertainty of the HITRAN line list and the continuum model.

The formula mentioned by the referee is already applied to the MUSICA (MAP) products. For simulating MUSICA NDACC and MUSICA IASI data with MAP a priori, we add $g^T(AK_{MUSICA} - I)(x_{apriori\_MUSICA} - x_{apriori\_MAP})$ to the MUSCIA NDACC and MUSICA IASI retrieval data, respectively.

g: column operator

AK_{MUSICA}: MUSICA averaging kernel (maps profiles to profiles)

I: Identity operator

$x_{apriori\_MUSICA}$: MUSICA a priori

$x_{apriori\_MAP}$: MAP a priori

MUSICA NDACC (MAP) and MUSICA IASI (MAP) products are calculated by adding this formula to the original MUSICA NDACC and IASI data. Therefore, the 1.13% difference between the two kinds of IASI datasets (MUSICA IASI and MUSICA IASI (MAP)) at Sodankylä mainly comes from the difference of a priori profiles (WACCM and MAP).

5) "Then, if the aposteriori correction seems to work for IASI, it could maybe be applied to TROPOMI to evaluate, how much of the Bias of the 9% might be explained due to the difference in the apriori. A plot of the average apriori of COCCON and TROPOMI might also help to evaluate this."

The a priori profiles for TROPOMI and COCCON on July 2, 2018 are presented in the figure below.

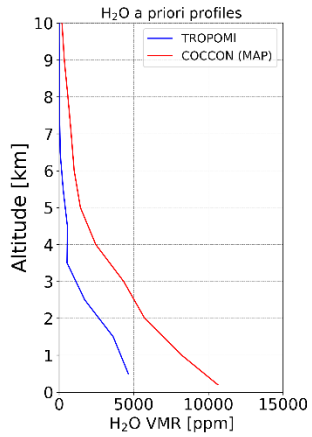

Could you generate posterior a TROPOMI(MAP) product? Or Just evaluate how much would the bias change?

Yes, this comment is a very good idea. We apply the function below to calculate the bias caused by the a priori profiles of TROPOMI and MAP:

$$\Delta XH_2O = \frac{\sum_{layers}^{i}\left(VMR_{TROPOMI(i)} - VMR_{COCCON(i)} * f\right) * subcol_{TROPOMI(i)} * \left(1 - AK_{TROPOMI(i)}\right)}{\sum_{layers}^{i} subcol_{TROPOMI(i)}}$$

$VMR_{TROPOMI}$ and VMR_{COCCON} are the a priori profiles of TROPOMI and COCCON. The COCCON retrievals are scaled to the a priori profiles by applying a single value. f is the ratio between the XH_2O integrated from the a priori profiles of TROPOMI and the XH_2O integrated from the a priori profiles of COCCON. $subcol_{TROPOMI}$ is the dry air sub-column of TROPOMI. $AK_{TROPOMI}$ is the column averaging kernel of TROPOMI.

The averaged relative bias $\left(2 \times \frac{\Delta XH_2O}{XH_2O_{COCCON} + XH_2O_{TROPOMI}} \times 100\%\right)$ is 1.15%. This value is similar to the relative bias change for MUSICA IASI at Sodankylä when applying different a priori profiles (1.13%).

6) I would actually ask the authors to include a typical averaging kernel of the two satellite products, maybe there is still space in Figure 5.

We add three subfigures to Figure 5 according to the referee's comment: TROPOMI averaging kernels, row averaging kernel of IASI and IASI correlation between DOFS and SZA. We use the row averaging kernel instead of column averaging kernel for IASI because MUSICA IASI is a profile retrieval and generates profiles with DOFS of 4-6.

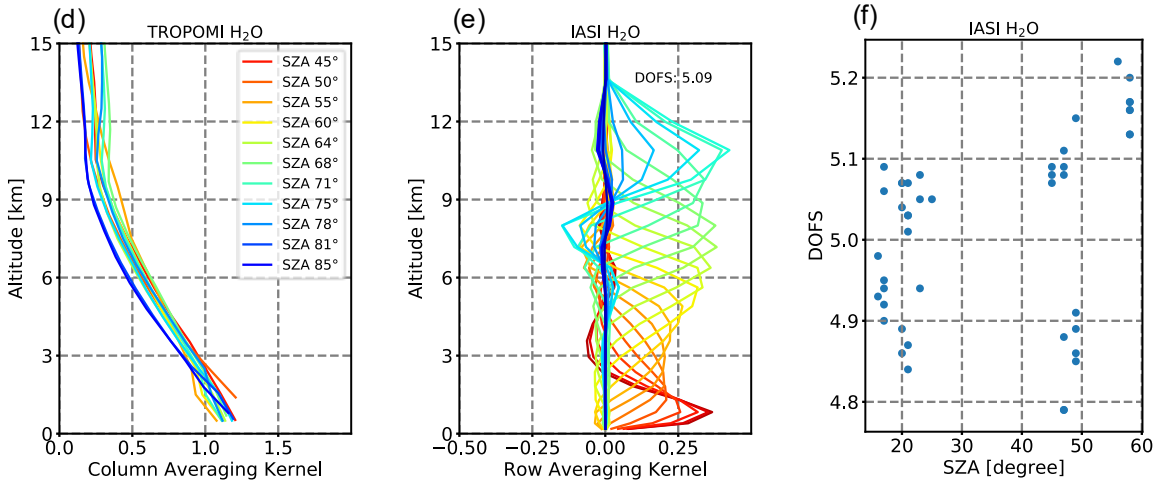
(d)
TROPOMI H_2O
SZA 45°
SZA 50°
SZA 55°
SZA 60°
SZA 64°
SZA 68°
SZA 71°
SZA 75°
SZA 78°
SZA 81°
SZA 85°
Altitude [km]
Column Averaging Kernel
(e)
IASI H_2O
DOFS: 5.09
Altitude [km]
Row Averaging Kernel
(f)
IASI H_2O
DOFS
SZA [degree]

Intercomparison of arctic XH_2O observations from three ground based FTIR networks and application for satellite validation

Qiansi Tu[1], Frank Hase[1], Thomas Blumenstock[1], Matthias Schneider[1], Andreas Schneider[2], Rigel Kivi[3], Pauli Heikkinen[3], Benjamin Ertl[1,4], Christopher Diekmann[1], Farahnaz Khosrawi[1], Michael Sommer[5], Tobias Borsdorff[2], Uwe Raffalski[6]

[1]Karlsruhe Institute of Technology (KIT), Institute of Meteorology and Climate Research (IMK-ASF), Karlsruhe, Germany
[2]SRON Netherlands Institute for Space Research, Utrecht, the Netherlands
[3]Finnish Meteorological Institute, Sodankylä, Finland
[4]Karlsruhe Institute of Technology, SCC, Karlsruhe, Germany
[5]GRUAN Lead Centre, Deutscher Wetterdienst, Lindenberg, Germany
[6]Swedish Institute of Space Physics, Kiruna, Sweden

Correspondence to: Qiansi Tu (qiansi.tu@kit.edu)

Abstract.

In this paper, we compare column-averaged dry-air mole fractions of water vapor (XH_2O) retrievals from COCCON (COllaborative Carbon Column Observing Network) with retrievals from two co-located high-resolution FTIR (Fourier transform infrared) spectrometers as references at two boreal sites, Kiruna, Sweden and Sodankylä, Finland from March 6 2017 to September 20 2019. In the framework of the NDACC (Network for the Detection of Atmospheric Composition Change) an FTIR spectrometer is operated in Kiruna. The H_2O product derived from these observations has been generated with the MUSICA (MUlti-platform remote Sensing of Isotopologues for investigating the Cycle of Atmospheric water) processor. In Sodankylä, a TCCON (Total Carbon Column Observing Network) spectrometer is operated, and the official XH_2O data as provided by TCCON are used for this study. The datasets are in good overall agreement, with COCCON data showing a wet bias of (49.20 ± 58.61) ppm ((3.33 ± 3.37) %, R^2=0.9992) compared to MUSICA NDACC and (56.32 ± 45.63) ppm ((3.44 ± 1.77) %, R^2=0.9997) compared to TCCON.

Furthermore, the a priori H_2O VMR (volume mixing ratio) profiles (MAP) used as a priori in the TCCON retrievals (also adopted for COCCON retrievals) are evaluated with respect to radiosonde (Vaisala RS41) profiles at Sodankylä. The MAP and radiosonde profiles show similar shapes and a good linear correlation of integrated XH_2O, indicating that MAP is a reasonable approximation for the true atmospheric state and an appropriate choice for the scaling retrieval methods as applied by COCCON and TCCON. COCCON shows a reduced dry bias (-14.96 %) in comparison to TCCON (-19.08 %) with respect to radiosonde XH_2O.

Finally, we investigate the quality of satellite data at high latitudes. For this purpose, the COCCON XH_2O is compared with retrievals from the Infrared Atmospheric Sounding Interferometer (IASI) generated with the MUSICA processor (MUSICA IASI) and with retrievals from the TROPOspheric Monitoring Instrument (TROPOMI). Both paired datasets show generally good agreement and similar correlations at the two sites. COCCON measures 4.64 % less XH_2O at Kiruna and 3.36 % at

Sodankylä with respect to MUSICA IASI, while COCCON measures 9.71 % more XH_2O at Kiruna and 7.75 % at Sodankylä compared with TROPOMI.

Our study supports the assumption that COCCON also delivers a well-characterized XH_2O data product. This emphasizes the approach of supplementing the TCCON network for satellite validation efforts. This is the first published study where COCCON XH_2O is compared with MUSICA NDACC and TCCON retrievals, and for MUSICA IASI and TROPOMI validation.

1. Introduction

Water vapor (H_2O) is among the most abundant gases in the atmosphere and nearly 99 % of the water vapor exists in the troposphere. It has a residence time of about nine days in the atmosphere (Trenberth, 1998) and absorbs approximately 57 % in the long-wave radiation and 72 % in the short-wave in clear skies (Kiehl and Trenberth, 1997). Due to its numerous absorption, atmospheric water vapor also acts as an important greenhouse gas (GHG). It plays a key role in the Earth's energy budget and the large-scale circulation, and thus the climate of our planet (Allan, 2012). Because the equilibrium water vapor pressure increases rapidly with temperature, the increasing atmospheric concentration of water vapor further amplifies warming due to its added radiative absorption (Soden et al., 2002). Therefore, assessing and quantifying atmospheric water vapor is essential to constrain weather and climate models.

The distribution of water vapor in the atmosphere is characterized by very high spatial and temporal variability relevant to weather and climate (Vogelmann et al., 2015). Satellite-borne instruments have the advantage of global coverage but lack of vertical or long-term information (Dupuy et al., 2016). Additionally, satellite water vapor data contain inherent uncertainties and must be validated before use (Loew et al., 2017). On the other hand, independent ground-based remote sensing instruments and in situ sensors do not give access to the global scale but can provide very accurate and long-term data, which can be used for satellite validation. Many studies have investigated water vapor comparisons among satellite and ground-based instruments (Schneider and Hase, 2011; Dupuy et al., 2016; Borger et al., 2018; Trieu et al., 2019), but there are only few studies that focus on the Arctic region (Pałm et al., 2010; Buehler et al., 2012; Alraddawi et al., 2018).

In this work, we present a comparison of column-averaged dry-air mole fractions of water vapor (XH_2O) retrievals from three ground-based networks, two space-borne satellites and vertical profiles from in situ radiosondes near Arctic region. This paper is organized as follows: Sect. 2 gives a description of the campaign sites and lists the details of the instruments. The datasets used in this study and coincidence criteria will be presented in Sect. 3. Results are discussed in Sect. 4 and 5, followed by conclusions in Sect. 6.

2. Ground-based and space-borne instrumentation

2.1 TCCON network

The Total Carbon Column Observing Network (TCCON) is a worldwide network of ground-based Fourier transform infrared (FTIR) spectrometers, measuring solar absorption spectra in the near infrared region. The TCCON network is designed to provide accurate and long-term time series of column-averaged dry-air mole fractions of greenhouse gases and other atmospheric constituents for carbon cycle studies and satellite validation (Wunch et al., 2011). The TCCON measurements have very high precision due to the minimal effect from surface properties and aerosols (Wunch et al., 2017). The TCCON sites are distributed globally, but with higher density in Europe, Northern America and eastern Asia. Its costs and high demand for qualified personnel and infrastructure hinder its expansion. Remote sites or regions with high or low surface albedo, which are also interesting for satellite and model validation are generally poorly covered by the TCCON stations.

TCCON data are retrieved by the non-linear least-squares fitting algorithm (GFIT). The GFIT algorithm scales a priori water vapor profiles from the National Centers for Environmental Prediction reanalysis data (https://www.ncdc.noaa.gov/data-access/model-data/model-datasets/reanalysis-1-reanalysis-2) to obtain a best-fit synthetic spectrum for the measured spectrum (Wunch et al., 2011). Some retrieval information for TCCON and other products used in this study are listed in Table A 1.

2.2 COCCON network and FRM4GHG campaign

Recently, a cheaper, robust and portable ground-based FTIR spectrometer (EM27/SUN) has been developed by the Karlsruhe Institute of Technology (KIT) in cooperation with the company Bruker (Gisi et al. (2012), Frey et al. (2015) and Hase et al. (2015, 2016)). The EM27/SUN instruments are characterized with good quality, robustness and reliability in several successful field campaigns (Frey et al., 2015; Klappenbach et al., 2015; Chen et al., 2016; Butz et al., 2017; Vogel et al., 2019; Sha et al., 2019; Tu et al., 2020; Jacobs et al., 2020) and their excellent level of performance opens up the chance of supporting the TCCON network. The spectrometers are commercially available since spring 2014 and today about 60 spectrometers are in operation around the world. KIT initiated the COllaborative Carbon Column Observing Network (COCCON, https://www.imk-asf.kit.edu/english/COCCON.php) as a framework for proper operation of the EM27/SUN spectrometer (Frey et al., 2019) and for ensuring common standards for data analysis. Each COCCON spectrometer (including the spectrometers operated in Kiruna and Sodankylä as used in this study) is checked and calibrated at the calibration facility operated in Karlsruhe (using a TCCON spectrometer and the primary EM27/SUN spectrometer unit) before shipment to the observation site. For the purpose of COCCON data processing, a preprocessing tool and the non-linear least-squares fitting algorithm PROFFAST have been created with the support of the European Space Agency (ESA) (projects COCCON-PROCEEDS and COCCON-PROCEEDS II). The EM27/SUN spectrometer offers a low spectral resolution of 0.5 cm^{-1} and consequently has little vertical resolution capability. Therefore, a simple least-squares fit performing a scaling retrieval of the a priori profile is generally appropriate and sufficient.

In this work, two COCCON instruments were operated at the Swedish Institute of Space Physics (IRF), Kiruna, Sweden (67.84° N, 20.41° E, 419 m a.s.l.) and at the Finnish Meteorological Institute (FMI), Sodankylä, Finland (67.37° N, 26.63° E, 181 m a.s.l.) since March 2017. The COCCON measurements in Finland are made in the frame-work of the FRM4GHG (Fiducial Reference Measurements for Ground-Based Infrared Greenhouse Gas Observations, http://frm4ghg.aeronomie.be/) campaign, funded by ESA ~~the European Space Agency (ESA)~~. This campaign aims at characterizing the performance of several low-cost and portable instruments for performing GHG measurements simultaneously in comparison with the TCCON retrievals at FMI, Finland (Sha et al., 2019). The dataset from this campaign will also serve for the TROPOspheric Monitoring Instrument (TROPOMI) validation and the campaign provides a guideline for establishing portable low-resolution FTIR spectrometers for complementing the TCCON network.

2.3 MUSICA NDACC products

The quality assessment study is also complemented by the MUSICA (MUlti-platform remote Sensing of Isotopologues for investigating the Cycle of Atmospheric water) dataset, including ground-based remote sensing, space-based remote sensing and in situ measurements (Schneider et al., 2012; Schneider et al., 2016). In this study, we focus on the first dataset.

Currently, there are 12 NDACC (Network for the Detection of Atmospheric Composition Change, http://www.acd.ucar.edu/irwg/, Kurylo and Zander, 2000; De Mazière et al., 2018) stations for which MUSICA NDACC datasets were created (Barthlott et al., 2017). The MUSICA NDACC retrievals are made by fitting 9 different spectral microwindows with water vapor signatures in the spectral region between 2655 and 3055 cm^{-1} using the PROFFIT retrieval code (PROFile FIT, Hase et al. 2004). The retrieval consists of an optimal estimation of the vertical distribution of H_2O, together with the ratios of different water vapor isotopologues. For all the retrievals a constant unique a priori profile is used, which is a global mean water vapor state, i.e. there is no variability in the a priori. This has the advantage that all detected variability is induced by the observation, but at the cost that the a priori profile can be rather off from the actual atmospheric state, which is a minor issue given the vertical sensitivity as revealed by the profile averaging kernels (Barthlott et al., 2017). Here we use MUSICA NDACC from the NDACC data base and perform a simple bias correction. This correction consists in adding A*c to the original data, where A is the averaging kernel in logarithmic scale and c a profile vector with the entry -0.12 for all altitudes. This means that we consider a bias of +12% in the original MUSICA H_2O data.

The PROFFIT code has been successfully used for many years in the ground-based FTIR community for evaluating high-resolution solar absorption spectra (Hase et al., 2004; Schneider and Hase, 2011). NDACC enables monitoring the distribution of a large variety of atmospheric trace gases in the mid-infrared region with Bruker HR120/5 FTIR spectrometers, including water vapor at a very high precision (Schneider et al., 2006; Schneider and Hase, 2009; Schneider et al., 2010a). The Kiruna NDACC observations are well representative for high latitudes and the MUSICA NDACC Kiruna data are available for the whole period from 1996 to present (Blumenstock et al., 2006).

2.4 MUSICA IASI products

The Infrared Atmospheric Sounding Interferometer (IASI) is the primary payload carried on the EUMETSAT's MetOp series of polar-orbiting satellites (Clerbaux, 2009), which provides a near-global distribution of observations with high resolution and accuracy twice a day. There are currently three IASI instruments in operation, which were launched in 2006, 2012 and 2018, respectively. The primary intent of IASI is to provide information on atmospheric temperature and water vapor, although several additional trace gases are accessible in the spectra.

The MUSICA NDACC retrievals are based on the retrieval code PROFFIT while the MUSICA IASI retrievals are based on a nadir version of PROFFIT (Schneider and Hase, 2009). The retrieval uses a single broad spectral window between 1190 and 1400 cm^{-1} and consists of a simultaneous optimal estimation of the vertical distribution of H_2O, the ratio of different water vapor isotopologues, N_2O, CH_4, and HNO_3. Atmospheric temperature is also fitted but constrained strongly to the EUMETSAT IASI Level 2 temperature product. For more details on the MUSICA IASI retrievals and the validation of the MUSICA IASI H_2O product please refer to Schneider et al. (2016) and Borger et al. (2018). The version presented here is an update as described by Borger et al. (2018) using a priori profiles for the gases under consideration, which depend on season and latitude. This dependency is determined from WACCM (Whole Atmosphere Community Climate Model) model simulations (a more detailed description of the new MUSICA IASI retrieval version is currently in preparation for ESSD (Earth System Science Data).

2.5 TROPOspheric Monitoring Instrument

The Tropospheric Monitoring Instrument (TROPOMI) is the single payload onboard the Sentinel-5 Precursor (S5P) satellite and was launched in October 2017 (Veefkind et al., 2012). It is a nadir-viewing grating spectrometer, covering the ultraviolet to shortwave infrared (SWIR) band. The SWIR module on TROPOMI has a spectral range of 4190 – 4340 cm^{-1}, a spectral resolution of 0.45 cm^{-1} and an unprecedented spatial resolution of 7 km × 7 km (5.5 km × 7 km after August 2019). A study from Schneider et al. (2020) shows a good agreement between the corrected TCCON H_2O column and co-located TROPOMI H_2O column, with a mean bias of $(-0.2 \pm 3) \times 10^{21}$ molec. cm^{-2} ((1.1 ± 7.2) %).

2.6 In situ radiosonde

Atmospheric profiles are regularly measured by meteorological radiosondes. In January – March 2017 Vaisala RS92 radiosondes (Dirksen et al., 2014) were launched at Sodankylä. The radiosonde system was upgraded in March 2017 and since late March 2017 Vaisala RS41 radiosondes have been launched at 23:30 UTC and 11:30 UTC daily. During special observing periods additional radiosondes have been launched at 05:30 UTC and 17:30 UTC. The regular radiosondes at Sodankylä have been launched using an automated launching system by Vaisala Oy since early 2006 (Madonna et al., 2020). Vaisala RS41 radiosonde contributes to improvements in accuracy and data consistency and its specifications for combined measurement uncertainties are 0.3 °C for temperature below 16 km and 0.4 °C above, 4 % RH for relative humidity, 1.0 hPa for pressure

larger than 100 hPa and 10 m for geopotential height (https://www.vaisala.com/sites/default/files/documents/RS-Comparison-White-Paper-B211317EN.pdf).

3. Datasets used and coincidence criteria

3.1 Ground-based datasets

In the present study, all datasets are obtained during the period from 2017 to 2019. We used the MUSICA NDACC XH_2O data from Kiruna (Barthlott et al., 2017) and the latest version GGG2014 TCCON XH_2O data from Sodankylä (Kivi and Heikkinen, 2016; Kivi et al., 2017) as references.

The COCCON and TCCON XH_2O is computed as the ratio of the co-retrieved total column of O_2 to an assumed dry-air mole fraction of O_2 equal to 0.2095 (Wunch et al., 2015):

$$XH_2O = \frac{TC_{H_2O}}{TC_{O_2}} \times 0.2095 \quad (1)$$

The total column of O_2 is not available from the NDACC network. Therefore, the XH_2O is calculated by dividing the total column of H_2O by the total column of dry air and the latter is computed from the surface pressure (P_s) recorded at a local weather station:

$$TC_{dryair} = \frac{P_s}{m_{dryair} \times g(\varphi)} - \frac{m_{H_2O}}{m_{dryair}} \times TC_{H_2O} \quad (2)$$

$$XH_2O = \frac{TC_{H_2O}}{TC_{dryair}} \quad (3)$$

where P_s is the surface pressure at Kiruna ground level, m_{dryair} and m_{H_2O} are the molecular masses of dry air ($\sim 28.96\ \mathrm{g \cdot mol^{-1}}$) and water vapor ($\sim 18\ \mathrm{g \cdot mol^{-1}}$), respectively, TC_{dryair} and TC_{H_2O} are the total column amount of dry air and water vapor, and $g(\varphi)$ is the latitude-dependent surface acceleration due to gravity.

The co-located COCCON measurements from Kiruna and Sodankylä are coincident with NDACC and TCCON measurement with hourly mean, respectively. Due to the high measurement frequency, the TCCON and COCCON measurements offer opportunities for estimating the water vapor intraday variability. To reduce the residual uncertainties introduced by airmass dependence, empirical corrections are applied by TCCON (Wunch et al., 2015) and COCCON. The solar zenith angle (SZA) range has been limited to 80°. This also reduces the collocation error with the satellite borne thermal nadir sounder IASI, whose typical nadir angle range is 0° – 48.3°.

3.2 Space-borne datasets

For space-borne data, a similar geophysical collocation criterion is used in this study as used in Schneider et al. (2020). The MUSICA IASI and TROPOMI data are collected within a radius of 30 km of the COCCON sites in Kiruna and Sodankylä with an acceptance cone of 45° width in the FTIR viewing direction and all ground-based measurements acquired within 30

min of each satellite overpass (before or after). To reduce the altitude effect, the satellite data are filtered for ground pixels with altitudes between 350 and 500 m a.s.l. for Kiruna and 100 and 250 m a.s.l. for Sodankylä, respectively (Kiruna and Sodankylä stations are located at 420 and 189 m a.s.l., respectively). For the TROPOMI data we also applied additional filters for reducing the effects of clouds and high aerosol. The cloud cover is limited to 1 % for both the inner and outer field of view (Schneider et al., 2020). The soundings with high aerosol load are filtered out with a two-band methane filter, when the difference between the retrieved methane in weak and strong absorption is larger than 6 % (Scheepmaker et al., 2016; Hu et al., 2018).

It is noted that the seasonal variation of atmospheric water vapor is large; therefore, we report the bias and also relative bias (in percent) for one pair of XH_2O datasets. The relative bias is calculated as below:

$$\boldsymbol{Rel.bias} = \mathbf{2} \times \frac{\boldsymbol{X_{gas\_A}} - \boldsymbol{X_{gas\_B}}}{(\boldsymbol{X_{gas\_A}} + \boldsymbol{X_{gas\_B}})} \times \mathbf{100}\,\% \tag{4}$$

3.3 Volume mixing ratio of H_2O derived from radiosonde measurements

The relative humidity (RH) measured by the in situ radiosondes is equivalent to the partial pressure of H_2O divided by the saturation vapor pressure of H_2O:

$$\boldsymbol{RH} = \frac{\boldsymbol{P_{H_2O}}}{\boldsymbol{e_s(T)}} \times \mathbf{100}\,\% \tag{5}$$

where P_{H_2O} is the partial pressure of H_2O, $e_s(T)$ is the saturation vapor pressure which only depends on temperature. Here we use the empirical equation from Hyland and Wexler (1983) to present e_s:

$$\boldsymbol{e_s} = \boldsymbol{exp}\left(\frac{-\mathbf{0.58002206} \times \mathbf{10^4}}{\boldsymbol{T}} + \mathbf{0.13914993} \times \mathbf{10} - \mathbf{0.48640239} \times \mathbf{10^{-1}} \times \boldsymbol{T} + \mathbf{0.41764768} \times \mathbf{10^{-4}} \times \boldsymbol{T^2} - \mathbf{0.14452093} \times \mathbf{10^{-7}} \times \boldsymbol{T^3} + \mathbf{0.65459673} \times \mathbf{10} \times \boldsymbol{log}(\boldsymbol{T})\right) \tag{6}$$

where T denotes the temperature in Kelvin.

The volume mixing ratio (VMR) of H_2O (VMR_{H_2O}) is defined as the ratio of partial pressure of H_2O (P_{H_2O}) relative to the total pressure (P):

$$\boldsymbol{VMR_{H_2O}} = \frac{\boldsymbol{P_{H_2O}}}{\boldsymbol{P}} \tag{7}$$

Combing Equations (5) – (7) allows the VMR of H_2O to be computed from radiosonde measurements of relative humidity, temperature and pressure:

$$\boldsymbol{VMR_{H_2O}} = \frac{\boldsymbol{RH} \times \boldsymbol{e_s(T)}}{\boldsymbol{P}} \tag{8}$$

where RH denotes the relative humidity, e_s denotes the saturation vapor pressure and P denotes the total pressure.

4. Comparison of Arctic COCCON XH_2O

We determine the precision by an intercomparison between COCCON and ground-based FTIR datasets. The XH_2O observed by the COCCON instruments at two sites is first compared with co-located ground-based MUSICA NDACC retrievals for Kiruna and with TCCON retrievals for Sodankylä, respectively. Furthermore, in situ radiosonde profiles at Sodankylä are used to investigate the a priori profile shape, and to evaluate TCCON and COCCON XH_2O data.

4.1 Seasonal variations of XH_2O

Time series of different datasets from 2017 (TROPOMI starting from 2018) to 2019 are depicted in Figure 1 for Kiruna and Sodankylä. COCCON measurements observes seasonal variations of XH_2O similar to the NDACC and TCCON measurements at each site. Here, we use additionally IASI and TROPOMI in the comparison and these datasets will be further discussed in Section 5. Multiple gaps are existing in the ground-based FTIR datasets due to poor weather and high SZA condition, while the FTIR measurements are performed under clear sky condition or during breaks in cloud cover. The number of MUSICA NDACC data is lower than the number of COCCON measurements due to the longer measuring time for NDACC compared to that of COCCON spectra and due to the use of optical filters by NDACC, which are recorded in sequence. The MUSICA NDACC data analyses use measurements recorded with one out of 6 optical filters used in the NDACC measurements.

In general, there are higher amounts of atmospheric XH_2O in summer then in spring and winter. For Kiruna, the amounts of XH_2O reach up to ~4000 ppm in each August 2017 and 2019 and even up to ~5500 ppm in August 2018, while there is only ~600 ppm XH_2O in each early spring and winter. Specific humidity shows a strong positive correlation with temperature (Issac and Wijngaarden, 2012). Meanwhile, the higher precipitation in summer intensifies the higher atmospheric water vapor concentration. The evaporation from the snow-covered continent and frozen water surface is still much less, limiting the transport of water vapor into the atmosphere. This effect lasts until spring due to the slow warming of the surface (Wypych et al., 2018). The XH_2O concentration is slightly higher at Sodankylä than at Kiruna, especially in summer. This is because the Sodankylä site (181 m a.s.l) has a lower altitude than the Kiruna site (419 m a.s.l), associated with enhanced contributions of humid atmospheric layers near ground to XH_2O.

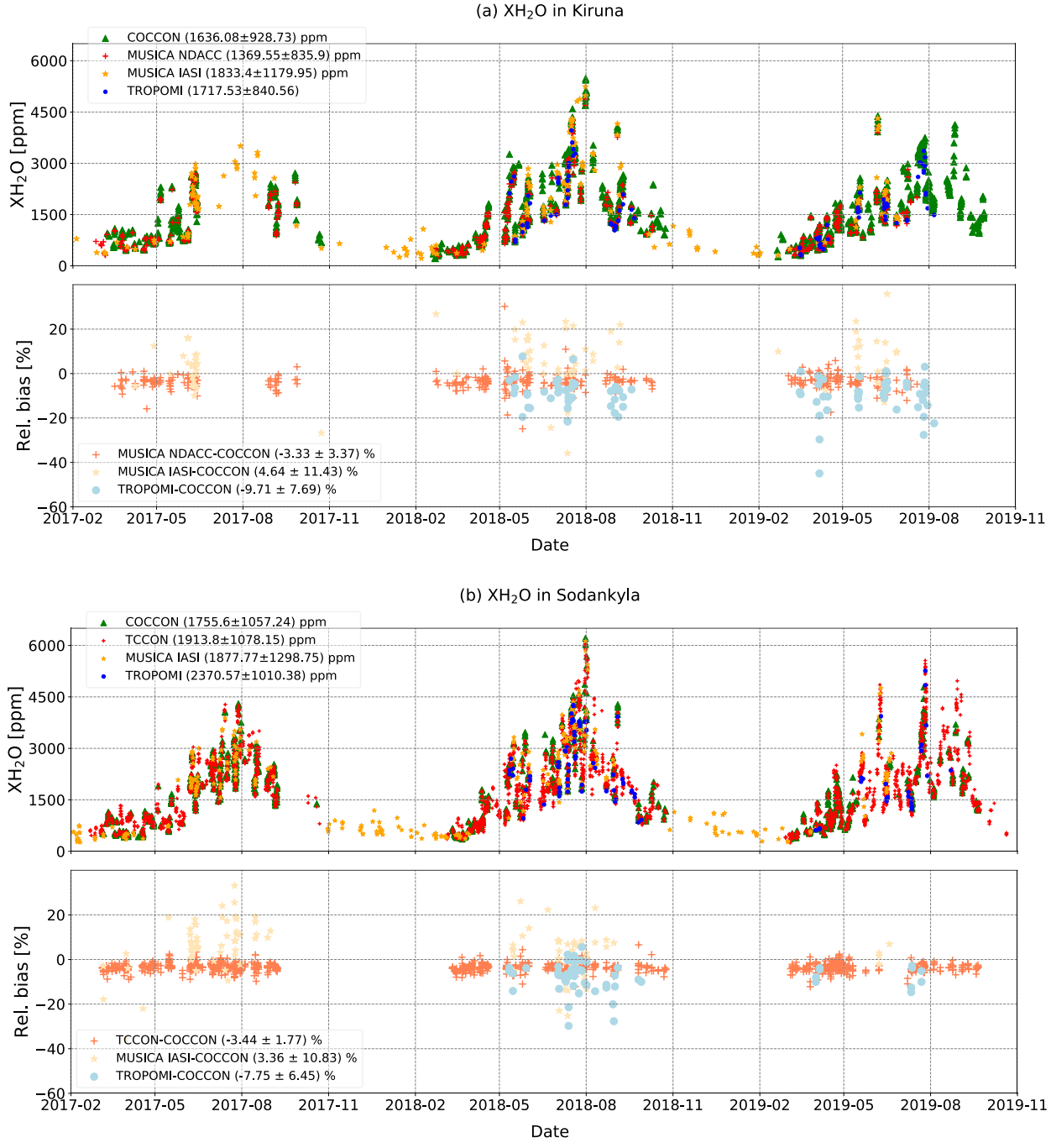

Figure 1. Time series of XH_2O derived from MUSICA IASI, TROPOMI, and ground-based FTIR instruments at (a) Kiruna and (b) Sodankylä. The corresponding relative biases are presented in the bottom panel for coincident pairs at each subfigure.

230

4.2 Comparison between COCCON and co-located ground-based FTIR instruments

Figure 2 gives the correlation of XH_2O measured by the COCCON instrument against coincident MUSICA NDACC retrievals for the Kiruna site (left) and against coincident TCCON retrievals for the Sodankylä site (right). In general, the two datasets at each site show quite good agreement and overall consistency, with R^2 value of 0.9992 for Kiruna and 0.9997 for Sodankylä. The second and seventh columns in Table 1 list the statistics for the coincident data between the COCCON and MUSICA NDACC XH_2O at the Kiruna site and between the COCCON and TCCON XH_2O at the Sodankylä site, respectively. Figure 3 shows the differences between the COCCON and the MUSICA NDACC retrievals at the Kiruna site and the differences between COCCON and TCCON retrievals at the Sodankylä site as a function of XH_2O amounts. There is no detectable dependence at both sites.

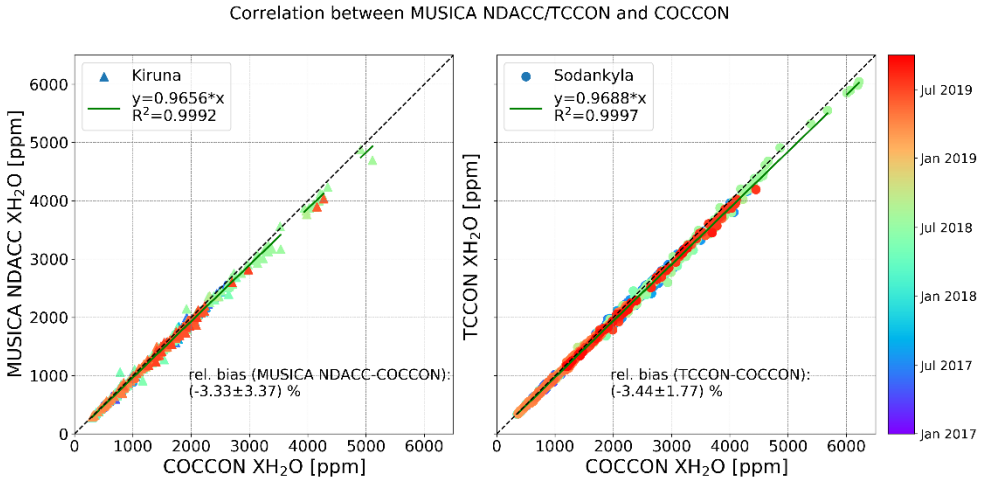

Figure 2. Correlation of COCCON XH_2O and coincident MUSICA NDACC retrievals for Kiruna (left) and of COCCON and coincident TCCON retrievals for Sodankylä (right). The solid green and dashed lines denote the linear fit and one-to-one lines, respectively. Color-coded from purple to red in order of measuring time from January 2017 to October 2019.

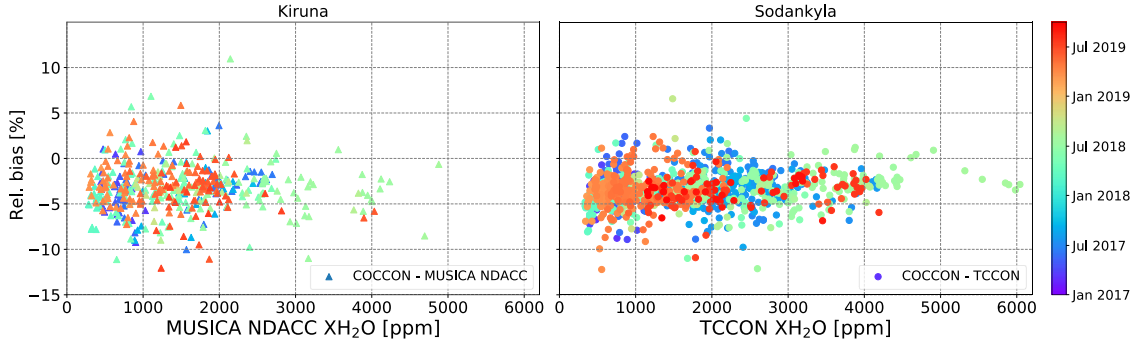

Figure 3. XH_2O difference (COCCON – MUSICA NDACC) for Kiruna (left) and XH_2O difference (COCCON – TCCON) for Sodankylä (right) versus XH_2O amounts. Color-coded from purple to red in order of measuring time from January 2017 to October 2019.

Figure 4 shows the XH_2O relative bias of MUSICA NDACC and TCCON compared to COCCON with respect to SZA over the whole period studied at the two stations. The absolute values of the relative bias between COCCON and MUSICA NDACC at Kiruna (left) show no obvious sensitivity to the SZA. However, the absolute value of the relative bias between COCCON and TCCON at Sodankylä becomes slightly larger with increasing SZA. This is because the TCCON and COCCON instruments have different spectral resolutions, which results in different absorption strengths and column averaging kernels (AVK) (Hedelius et al., 2016). Furthermore, the AVK also shows different sensitivity to the SZA of the measurement (Wunch et al, 2011). The AVK describes the sensitivity of the H_2O retrieval to a perturbation in the H_2O column at a given altitude. An AVK close to unity indicates maximum retrieval accuracy and an AVK larger or smaller than 1 indicate overestimation and underestimation of the true H_2O column amount, respectively.

Figure 5 depicts examples of AVKs for H_2O under different SZA on July 2nd, 2018. It reveals a sensitivity of very close to 100% for the lowermost altitudes, where most water vapor resides. The AVK for MUSICA NDACC H_2O retrievals shows no obvious sensitivity to the SZA and altitude, and are very close to unity below 5 km. However, TCCON and COCCON AVK vary with SZA and altitude. The TCCON AVKs are smaller than 1 and increases with increasing SZA below 1.5 km, and are larger than 1 and decrease with increasing SZA upwards. This change indicates that the TCCON H_2O total column underestimates a deviation near the surface and overestimates a deviation at higher levels from the a priori profiles. The COCCON AVKs show an opposite way, with overestimations and increasing value with larger SZA below 2 km, and with underestimations and decreasing value with larger SZA upwards. The overall column sensitivities of TCCON increase with increasing altitude, while the column sensitivities of COCCON decrease with increasing altitude. TROPOMI AVKs show a decrease trend as the increasing altitude, which is similar to the COCCON AVKs. However, no obvious SZA-dependent is observed in TROPOMI AKVs. Here, an example of row AVKs at SZA = 45° and degree of freedoms (DOFS) = 5.09 is presented for IASI (Figure 5 (e)) and DOFS shows a positive correlation to the SZA (Figure 5 (f)).

~~The AVKs for IASI and TROPOMI are not shown here but can be found in Borger et al., 2018 and Schneider et al., 2020, respectively.~~

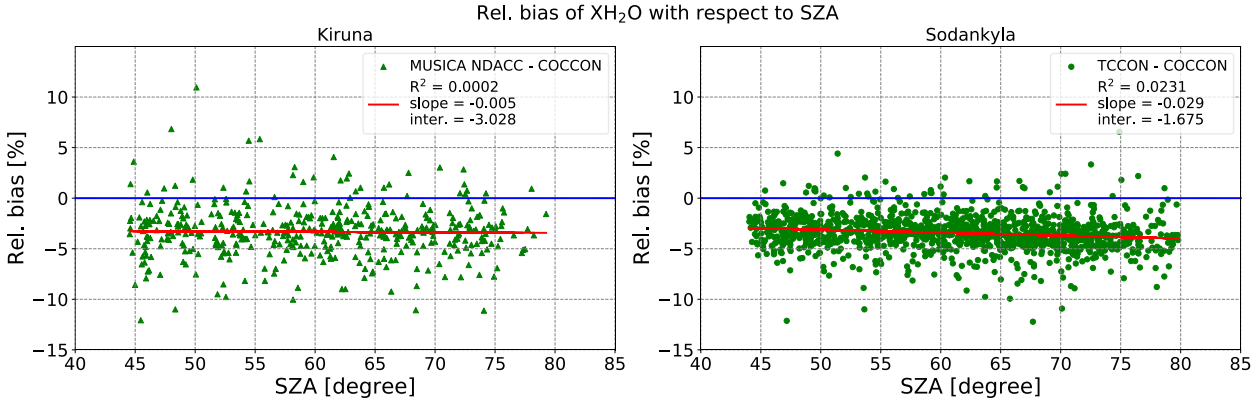

Figure 4. Dependence of the XH_2O difference (MUSICA NDACC – COCCON) at Kiruna site (left) and the difference (TCCON – COCCON) at Sodankylä site (right) on the SZA. The solid red line represents the fitting line.

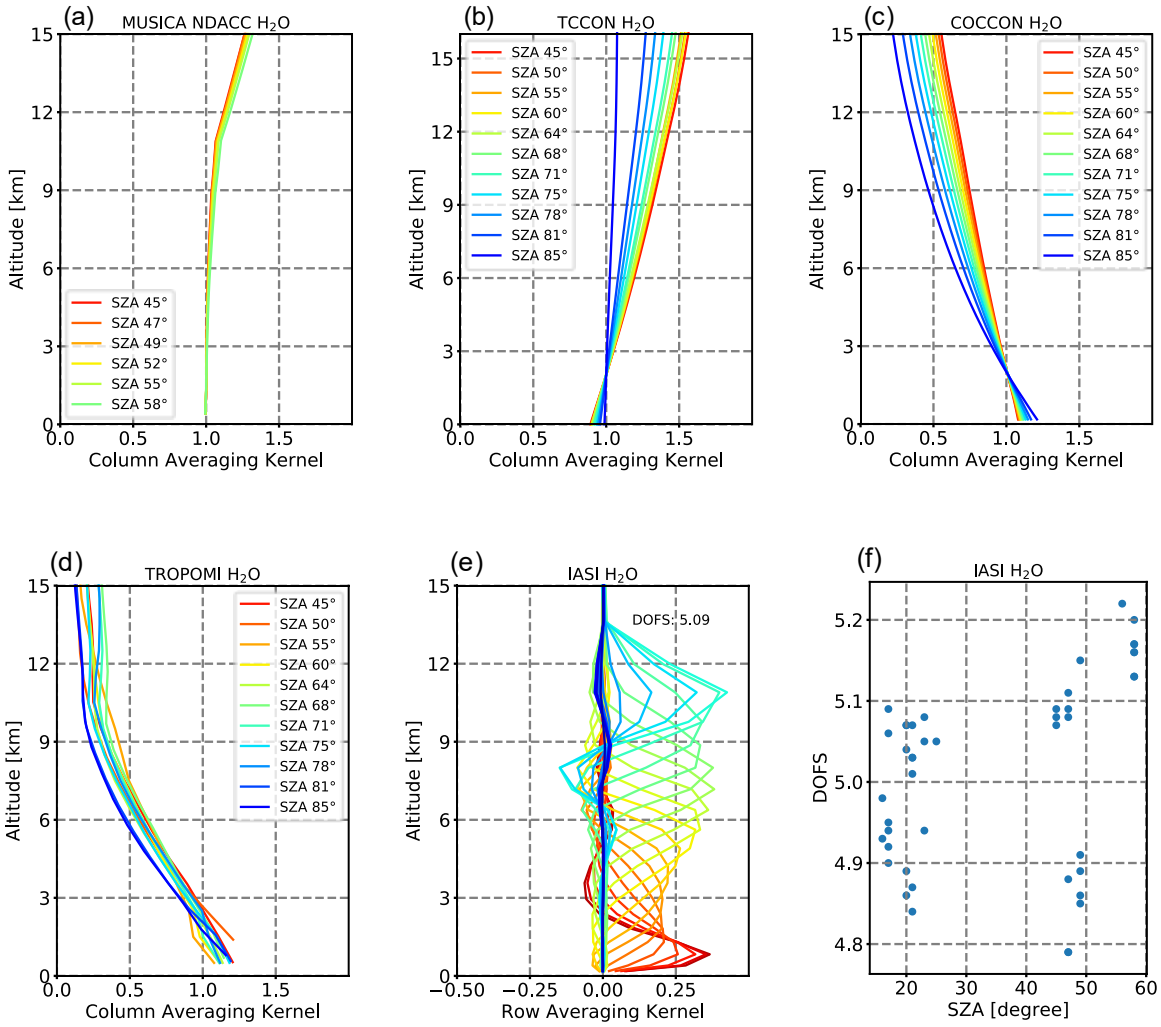

Figure 5. Examples of column averaging kernels for H_2O from (a) MUSICA NDACC, (b) TCCON, (c) COCCON and (d) TROPOMI for different SZA, (e) examples of row averaging kernel from IASI at DOFS=5.09 and (f) the correlation between SZA and DOFS for IASI on July 2nd, 2018.

Table 1. Statistical comparison between COCCON XH_2O and other instruments at each site. The total number of coincident data (No.) is listed. The biases and relative biases are presented in terms of mean value followed by standard deviation.

	Kiruna					Sodankylä			
	MUSICA NDACC	MUSICA NDACC (MAP)	MUSICA IASI	MUSICA IASI (MAP)	TROPOMI	TCCON	MUSICA IASI	MUSICA IASI (MAP)	TROPOMI
No.	505		101		87	1355	121		59

R^2	0.9992	0.9989	0.9904	0.9901	0.9950	0.9997	0.9917	0.9914	0.9961
Linear fit slope	0.9656	0.9776	1.0296	1.0404	0.9078	0.9688	1.0211	1.0375	0.9289
bias (ppm)	-49.20 ± 58.61	-24.45 ± 63.03	82.72 ± 233.35	108.54 ± 238.89	-176.55 ± 161.0	-56.32 ± 45.63	84.67 ± 251.	127.34 ± 257.81	-192.1 ± 179.49
relative bias (%)	-3.33 ± 3.37	-0.9 ± 4.31	4.46 ± 11.43	6.03 ± 11.59	-9.71 ± 7.69	-3.44 ± 1.77	3.36 ± 10.83	4.49 ± 10.86	-7.75 ± 6.45

When directly comparing the measurements from different remote sensing instruments, the differing observing system characteristics, particularly vertical sensitivity and a priori profiles should be considered (Rodgers and Connor, 2003). The COCCON instrument uses the same a priori H_2O VMR profiles as used in the TCCON network, derived from the National Centers for Environmental Prediction/National Center for Atmospheric Research (NCEP/NCAR) 6-hourly reanalysis data. A daily profile has been generated from the NCEP/NCAR data, interpolated to latitude, longitude and local solar noon time at the site. We refer to the TCCON a priori profiles as "MAP" files, following the naming convention used for the TCCON processing. MUSICA NDACC uses a single global climatology profile as a priori, which has no seasonal variations.

To assess the impact of the a priori profiles on the retrievals, the MAP a priori profiles used in TCCON and COCCON are applied to the MUSICA NDACC retrievals and IASI retrievals. We use MUSICA NDACC (MAP) and IASI (MAP) to represent the corresponding XH_2O to distinguish the official MUSICA NDACC and MUSICA IASI data. The MUSICA IASI (MAP) will be discussed in Section 5.1.

The correlation between MUSICA NDACC and MUSICA NDACC (MAP) and the time series of their relative bias are presented in Figure 6 (left panel). The MUSICA NDACC (MAP) XH_2O shows an excellent agreement with the MUSICA NDACC, with an R^2 value of 0.9998. When using the MAP profiles, the XH_2O retrievals are 2.57 % (standard deviation: 2.85 %) wetter than the MUSICA NDACC retrievals and higher relative biases are found early in the year when the atmosphere is dryer. This a priori choice increases slightly the correlation between MUSICA NDACC (MAP) and COCCON retrievals with the R^2 value of 0.9989 and consequently the relative difference decreases to –0.92 % (standard deviation: 4.31%). This small change indicates that MUSICA NDACC XH_2O has little sensitivity to the a priori information and the bias between MUSICA NDACC and COCCON is mainly due to the choices for the calibration of the XH_2O data product by either network.

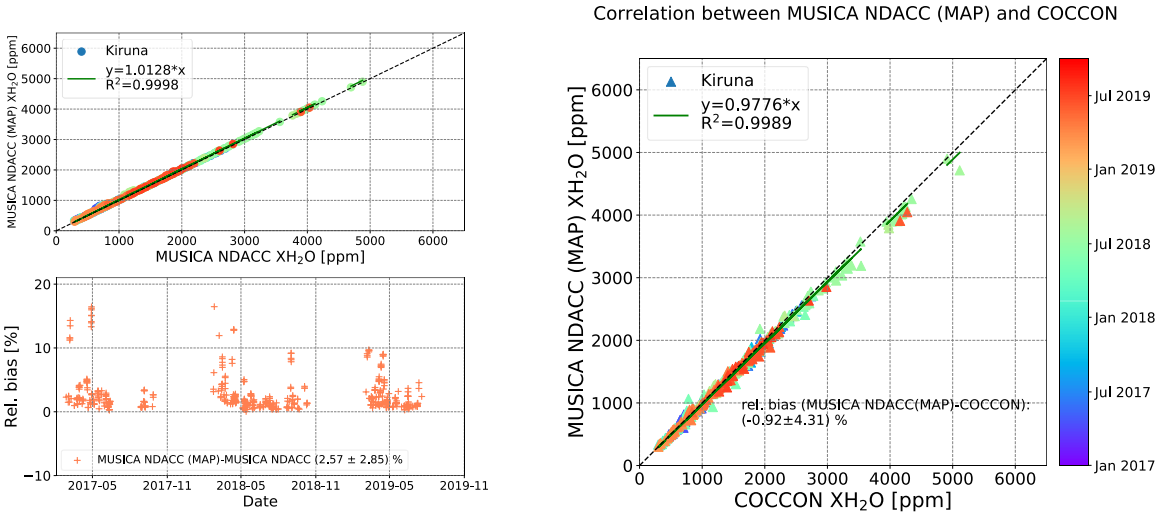

Figure 6. Correlation plot of MUSICA NDACC XH_2O and MUSICA NDACC (MAP) (top left), time series of their relative bias (bottom left), and correlation plot of COCCON XH_2O and coincident MUSICA NDACC (MAP) retrievals (right) at Kiruna site. The annotations follow those in Figure 2.

4.3 H_2O VMR profiles from in situ radiosonde at Sodankylä site

The comparison of the a priori H_2O profile used for the different instruments with in situ climatological knowledge of H_2O vertical variability yields a precision estimate for the retrievals. In this section, the MAP a priori profiles used in TCCON and COCCON are discussed using Vaisala RS41 radiosonde profiles as a reference.

The radiosondes are daily launched and the coincident MAP and radiosonde profiles cover nearly the whole year. Since most of the H_2O is located in the troposphere, we here present the profiles below 10 km. Figure 7 depicts the yearly-averaged H_2O VMR profiles derived from the MAP and Vaisala RS41 radiosonde (left panel) and the monthly-averaged relative biases between MAP and radiosonde profiles (right panel) for 2018. The ensemble of radiosonde profiles has a higher vertical resolution and is regridded to the lower vertical resolution of MAP profiles. The statistics of yearly-averaged MAP and radiosonde profiles at each level in 2018 are listed in Table 2.

The vertical H_2O VMR profiles of MAP are overestimated by 16.4 % at an altitude of 0.2 km with respect to the radiosonde profiles. The MAP profiles are generally closer to the radiosonde profiles between 1 – 4 km with a relative bias in the range of 1.1 % – 4.4 %. For the upper layers (above 4 km) MAP shows overall higher overestimations of H_2O (up to 19.4 %) than at the lower layers.

The time series of XH_2O from integrating the a priori MAP profiles and radiosonde profiles between 0.2 and 15 km is presented in Figure 8. These integrated-profile XH_2O shows similar seasonal variability as observed by COCCON and TCCON at Sodankylä. A good agreement is found for the integrated XH_2O between MAP and radiosonde profiles, with a relative bias of 3.95 % and a R^2 value of 0.9904 (Figure 9 (a)), indicating that the modeled MAP profiles can well represent the vertical variability of H_2O in the real atmosphere. TCCON measures 19.08 % drier XH_2O than the radiosonde with a R^2 value of

0.9952. There is a smaller dry bias in the COCCON XH_2O with respect to radiosonde and amounts to 14.96 % (R^2 = 0.9957). This high bias is mainly because COCCON and TCCON measures the total column of H_2O, while the radiosonde XH_2O is integrated up to 15 km and there are remaining H_2O above this level. ~~The small bias between COCCON and radiosonde indicates that COCCON is capable to serve for the validation of space-borne XH_2O measurements with useful accuracy.~~ ~~The estimated bias of MUSICA NDACC at Kiruna with respect to radiosonde is about −4.86 %.~~

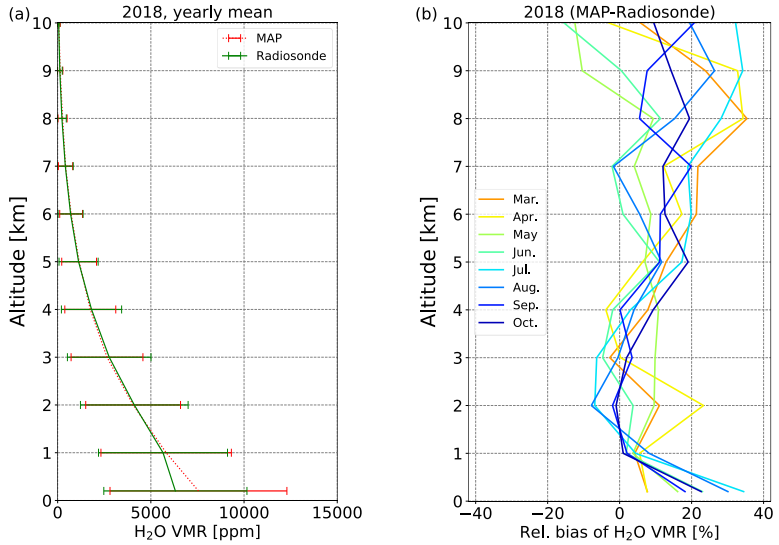

Figure 7. (a) Yearly-averaged H_2O VMR profiles as a function of altitude retrieved from MAP (in red) and the Vaisala RS41 radiosondes (in green) around noon at Sodankylä site in 2018 (the error bar denotes the standard deviation). (b) The corresponding monthly-averaged relative bias between MAP and radiosonde profiles. Vaisala RS41 radiosonde profiles are regridded to the vertical resolution of MAP profiles.

Table 2. Yearly mean and standard deviation for a priori MAP and radiosonde profiles at each level in 2018 and for their corresponding relative biases.

Height (km)	MAP (ppm)	Radiosonde (ppm)	Rel. bias (%) MAP-Radiosonde
0.2	7554 ± 4745	6315 ± 3840	16.38 ± 18.85
1	5821 ± 3499	5652 ± 3461	3.65 ± 12.34
2	4048 ± 2543	4110 ± 2888	4.84 ± 24.55
3	2647 ± 1927	2766 ± 2242	1.06 ± 26.11
4	1751 ± 1367	1817 ± 1615	4.37 ± 32.23
5	1152 ± 933	1122 ± 1049	10.65 ± 35.54
6	722 ± 611	694 ± 671	12.33 ± 36.71
7	423 ± 383	411 ± 424	9.44 ± 40.21
8	263 ± 243	228 ± 234	19.41 ± 39.57
9	136 ± 141	116 ± 131	14.11 ± 52.02

10	63 ± 77	53 ± 63	5.43 ± 52.02

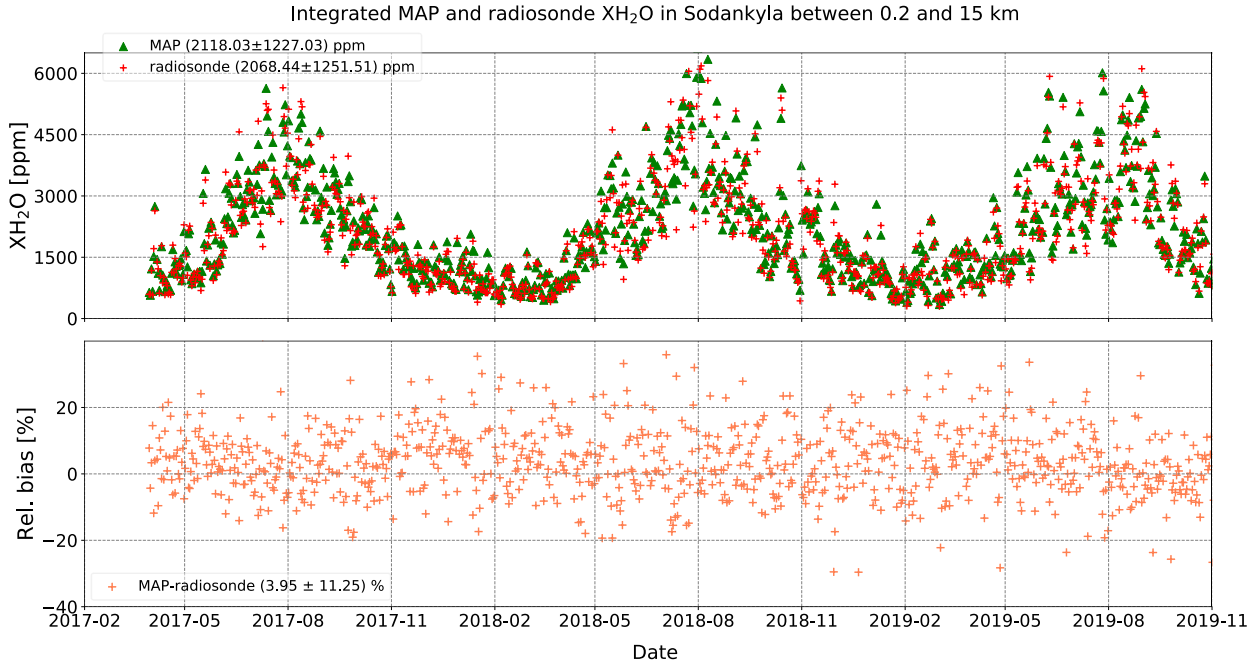

Figure 8. Time series of integrated XH_2O derived from MAP and radiosonde H_2O VMR profiles between 0.2 and 15 km. The corresponding relative biases are presented in the bottom panel.

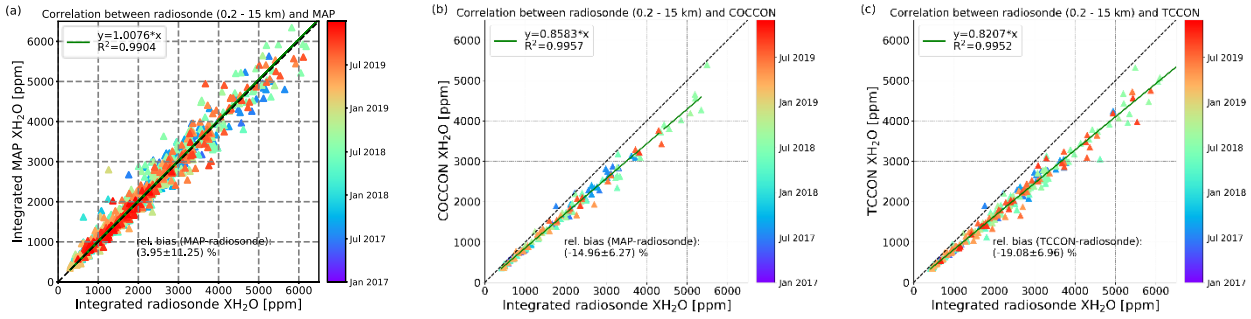

Figure 9. Correlation plots of the XH_2O derived from (a) MAP VMR profiles, (b) COCCON and (c) TCCON with respect to the XH_2O derived from coincident radiosonde profiles between 0.2 and 15 km at Sodankylä site. The annotations follow those in Figure 2.

5. Validation of satellite XH_2O data using COCCON as the reference

5.1 Comparison between COCCON and MUSICA IASI

The agreements between the IASI and COCCON retrievals at two sites are presented in Figure 10. COCCON XH_2O shows overall very good agreement with the MUSICA IASI data at both sites. For the Kiruna site COCCON measures a drier XH_2O than MUSICA IASI with a mean bias of 82.72 ppm (4.64 %) and a standard deviation of 234.56 ppm (11.43 %). COCCON measures a drier XH_2O at Sodankylä with a mean bias of 84.67 ppm (3.36 %) and a standard deviation of 252.26 ppm (10.83 %) with respect to MUSICA IASI. The coincident data between COCCON and MUSICA IASI show higher variations (standard deviation) than the coincident data between COCCON and ground-based MUSICA NDACC and TCCON. This is mainly because the IASI data is collected from a wide area around the ground-based FTIR stations and the varying altitudes also introduce additional biases. Partly cloudy conditions introduce biases to the IASI measurements, even if the cloud filter is applied. The fourth and eighth columns in Table 1 list the statistics between the coincident MUSICA IASI and COCCON XH_2O data at two sites.

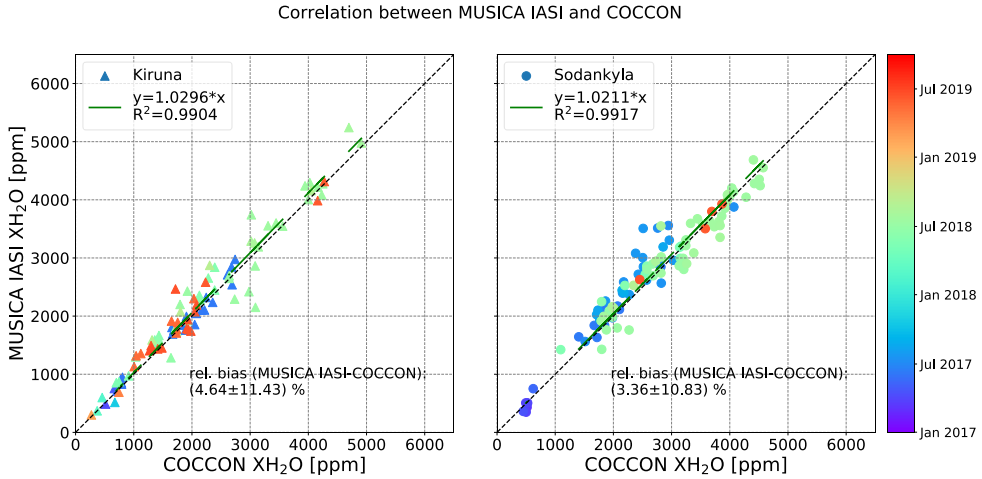

Figure 10. Scatter plot of the COCCON XH_2O compared to coincident MUSICA IASI retrievals at Kiruna site (left) and Sodankylä site (right). The annotations follow those in Figure 2.

Similar to the MUSICA NDACC (MAP) XH_2O, the application of MAP as a priori profiles does not impact the MUSICA IASI (MAP) too much. Figure 11a and b illustrate the correlations between the MUSICA IASI (MAP) and MUSICA IASI and the time series of their relative biases at Kiruna and Sodankylä. The two datasets at each site show an excellent agreement, with the same R^2 value of 0.9999. The MUSICA IASI (MAP) XH_2O is larger by 1.34 % and 0.96 % compared to MUSICA IASI retrievals at Kiruna and Sodankylä, respectively. These wetter retrievals result in increases in the relative biases between MUSICA IASI (MAP) and COCCON to 6.03 % at Kiruna and to 4.94 % at Sodankylä, respectively. In general, MUSICA IASI (MAP) also agrees very well with COCCON (see Figure 11c) similar to the correlation between MUSICA IASI and

COCCON, which reveals that the a priori profiles have small impact on the MUSICA IASI XH_2O and the bias between MUSICA IASI and COCCON is mainly due to the choices for the calibration of XH_2O data product by either dataset ~~network~~.

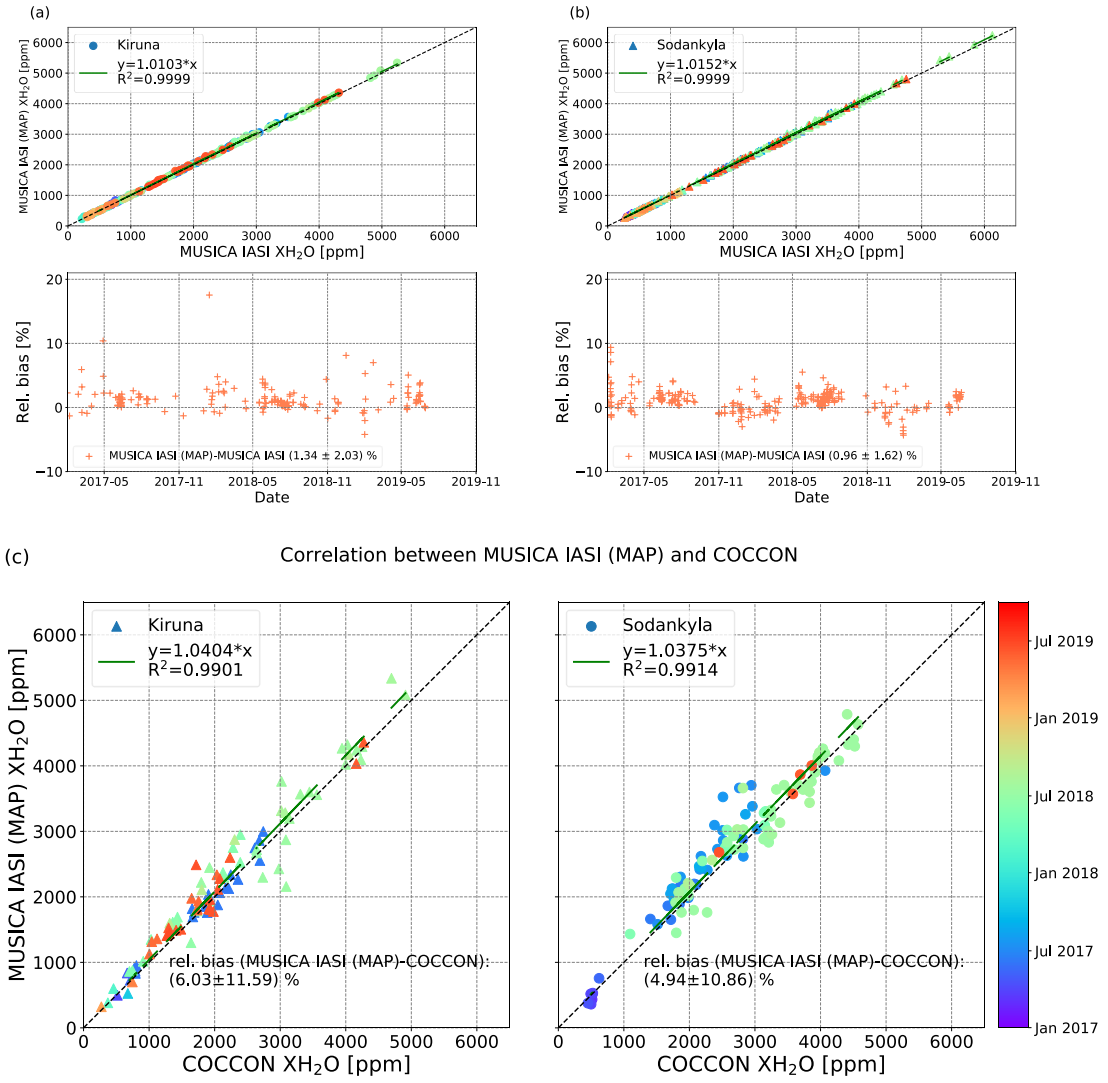

Figure 11. Correlation plots of MUSICA IASI XH_2O and MUSICA IASI (MAP) and time series of their relative difference at Kiruna site (a) and Sodankylä site (b), and correlation plot of COCCON XH_2O and coincident MUSICA IASI (MAP) retrievals at two sites (c). The annotations follow those in Figure 2.

5.2 Comparison between COCCON and TROPOMI ~~TROPOMI and COCCON~~

The correlation plots between TROPOMI and COCCON XH_2O data at Kiruna and Sodankylä sites are presented in Figure 12 and the sixth and tenth columns in Table 1 list the statistics for each site. The TROPOMI XH_2O shows generally good agreement with COCCON data and the correlations at both sites are similar. The slope demonstrates an underestimation of the TROPOMI retrievals vs. COCCON retrievals, with a factor of 0.9078 in Kiruna and 0.9289 in Sodankylä. The total bias is –

176.55 ppm (–9.71 %) with a standard deviation of 161.0 ppm (7.69 %) and the correlation coefficient is 0.9950 at Kiruna. The correlation at Sodankylä is slightly better, with a correlation coefficient of 0.9961, a mean bias of –192.1 ppm (–7.75 %), and a standard deviation of 179.49 ppm (6.45 %).

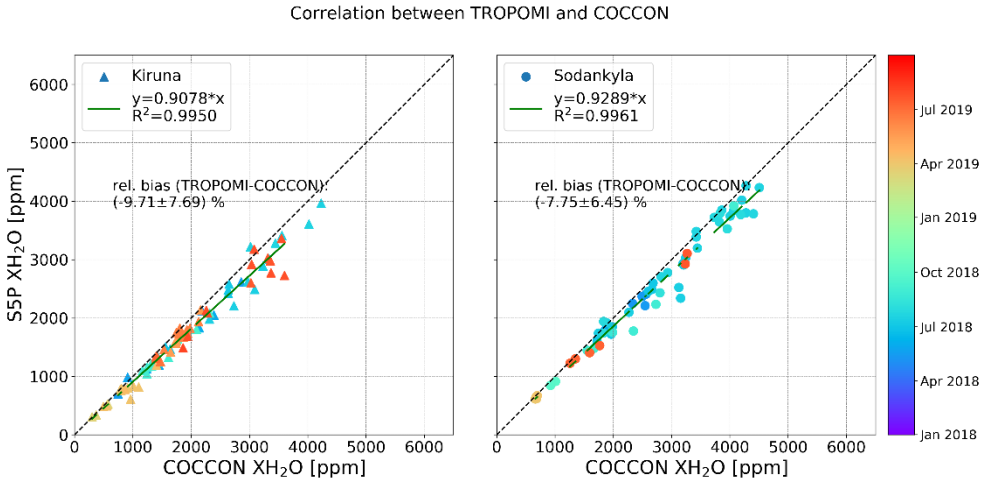

Figure 12. Correlation plots of TROPOMI and COCCON XH_2O at Kiruna site (left) and Sodankylä site (right). The annotations follow those in Figure 2. Noted that the color bar is from January 2018 to October 2019.

6. Summary and conclusions

In this paper, we compare the column-averaged dry-air mole fractions of water vapor (XH_2O) retrievals from COCCON and MUSICA NDACC at Kiruna and from COCCON and TCCON at Sodankylä during the period of 2017 – 2019. Additionally, we evaluate the vertical water vapor VMR profiles (MAP) as a priori used in COCCON and TCCON retrievals with in situ profiles retrieved from the radiosonde Vaisala RS41.

We found a very good agreement between the COCCON and the MUSICA NDACC data at Kiruna and between the COCCON and the TCCON data at Sodankylä. The COCCON retrievals have a tendency toward a wet bias of (–49.20 ± 58.61) ppm ((–3.33 ± 3.37) %) at Kiruna and (–56.32 ± 45.63) ppm ((–3.44 ± 1.77) %) at Sodankylä. The relative bias between COCCON and MUSICA shows no obvious sensitivity to the SZA, whereas, the absolute value of the relative bias between COCCON and TCCON becomes slightly larger with increasing SZA over 70°. This is because the TCCON and COCCON instruments have different spectral resolutions, which results in different absorption strengths and also averaging kernels (Hedelius et al., 2016).

The a priori profiles play an important role in the retrievals. The in situ measured vertical H_2O VMR profiles performed at Sodankylä provide the possibility to evaluate the a priori profiles (MAP) used in both COCCON and TCCON datasets. Since the shapes of profiles are similar over the years, we investigate the profiles in 2018 as an example. The difference between the MAP and radiosonde profiles varies with season and height, and higher differences are found near the surface in summer. The XH_2O amounts integrated from MAP and radiosonde profiles between 0.2 km to 15 km show a very good agreement (R^2 =

0.9904), indicating that MAP profiles are reasonably modeled and represent the vertical variability well. Compared to radiosonde, both COCCON and TCCON measure drier XH_2O with mean biases of 14.96 % and 19.08 %, respectively. These high biases are mainly because COCCON and TCCON measures the total column of H_2O, while the radiosonde XH_2O is only integrated up to 15 km and there are remaining H_2O above this level. ~~The small bias in COCCON with respect to radiosonde indicates that COCCON is capable to be serve for the validation of space-borne XH_2O measurements with useful accuracy. An estimated bias between MUSICA NDACC at Kiruna and radiosonde is about –4.86 %.~~

Secondly, comparisons between the COCCON and MUSICA IASI datasets at Kiruna and Sodankylä are also carried out and they show overall good agreement. COCCON measures a drier XH_2O against MUSICA IASI with a mean bias of 82.72 ppm (4.46 %) at Kiruna and with a mean bias of 84.67 ppm (3.36 %) at Sodankylä. However, COCCON measures a wetter XH_2O against TROPOMI data with a mean bias of –176.55 ppm (–9.71 %) at Kiruna and with a mean bias of –192.1 ppm (–7.75 %) at Sodankylä. The higher biases between COCCON and satellites is mainly because the satellite data are collected from a wide area around the ground-based FTIR stations and the varying altitudes also add a bias.

To assess the effect of the a priori profile, we also use the MAP profiles as a priori profiles for retrieving the MUSICA NDACC and MUSICA IASI XH_2O. The MUSICA NDACC (MAP) and MUSICA IASI (MAP) agree very well with their original dataset ($R^2 \geq 0.9998$), with no significant seasonal variations. When applying the MAP a priori profiles, we observe an overall increase in MUSICA NDACC (MAP) by 2.57 % in Kiruna, and an increase in MUSICA IASI (MAP) by 1.34 % in Kiruna and by 0.96 % in Sodankylä, respectively. Therefore, MUSICA NDACC and MUSICA IASI XH_2O show small sensitivity to the a priori profiles. The small biases between the MUSICA NDACC and COCCON and between MUSICA IASI and COCCON are mainly from the calibration choices of the XH_2O data product.

During this field campaign the low-cost and portable COCCON instrument shows its advantage of robustness, stability and reliability, which provides the potential to complement the TCCON network and for satellite validation. This is the first published study where COCCON XH_2O is compared with MUSICA NDACC and TCCON retrievals, and for MUSICA IASI and TROPOMI validation. Therefore, COCCON instrumentation may also serve as validation tool for space-borne XH_2O measurements, additionally to XCO_2 and XCH_4.

Author contributions. Frank Hase, Matthias Schneider and Qiansi Tu developed the research question. Qiansi Tu wrote the manuscript and performed the data analysis with support from Frank Hase, Thomas Blumenstock, Matthias Schneider, Andreas Schneider, Rigel Kivi, Pauli Heikkinen and Michael Sommer. Qiansi Tu, Thomas Blumenstock, Pauli Heikkinen, Rigel Kivi and Uwe Raffalski took an active part in the field campaign by operating the COCCON spectrometers and collecting data. Rigel Kivi and Pauli Heikkinen also operate the TCCON station at Sodankylä site and provided data. Andreas Schneider and Tobias Borsdorff provided the TROPOMI satellite data and gave technical support for the analysis. Matthias Schneider, Benjamin Ertl, Christopher Diekmann, and Farahnaz Khosrawi provided the MUSICA data. All authors discussed the results and contributed to the final manuscript.

Data availability. The TCCON GGG2014 data are publicly available from the TCCON Data Archive (https://doi.org/10.14291/tccon.ggg2014.sodankyla01.r0/1149280, Kivi et al., 2014). MUSICA NDACC data are available from ftp://ftp.cpc.ncep.noaa.gov/ndacc/MUSICA/. Global MUSICA IASI data will very soon be publicly available, since then they can be requested by email from Matthias Schneider. The S5P dataset is available at ftp://ftp.sron.nl/open-access-data-2/TROPOMI/tropomi/hdo/9_1/.

Competing interests. The authors declare that they have no conflict of interest.

Acknowledgements. The work presented here overlaps with the Fiducial Reference Measurements for Ground-Based Infrared Greenhouse Gas Observations (FRM4GHG) project funded by European Space Agency under the grant agreement number ESA-IPL-POE-LG-cl-LE-2015-1129. The MUSICA NDACC retrievals at Kiruna for the 2015-2019 time period have been made in the framework of the ESA S5P+I - H2O-ISO project (ESA/Contract No. 4000127561/19/I-NS). We also acknowledge ESA support through the COCCON-PROCEEDS and COCCON-PROCEEDS II projects. Funding from the Deutsche Forschungsgemeinschaft via the projects MOTIV and TEDDY (GZ: SCHN 1126/2-1 and GZ: SCHN 1126/5-1, respectively) enabled us to optimize the MUSICA IASI retrieval processing chain. The MUSICA IASI retrievals were performed on the supercomputer ForHLR funded by the Ministry of Science, Research and the Arts Baden-Württemberg and by the Federal Ministry of Education and Research.

The article processing charges for this open-access publication were covered by a Research Centre of the Helmholtz Association.

Appendix

Table A 1. Parameters of different instruments used in this study.

	COCCON	TCCON	MUSICA NDACC	MUSICA IASI	TROPOMI
Spectral window (cm^{-1})	8353.4 – 8463.1	6076.90 – 6469.60 (Wunch et al., 2010)	2658 – 3053	1190 – 1400	4200.8 – 4248.1 (Scheepmaker et al., 2016)
Spectroscopic modelling	HITRAN 2009	HITRAN 2009	HITRAN 2012 with modifications to consider speed-dependent Voigt line shapes (Barthlott et al., 2017)	HITRAN 2016, Voigt line shapes Water vapor continuum model: MT_CKD v2.5.2 (Delamere et al., 2010; Payne et al., 2011; Mlawer et al., 2012)	HITRAN 2016
A priori H_2O	NCEP/ NCAR[1]	NCEP/ NCAR	Globally mean WACCM[2] profile. No latitudinal and seasonal dependence	Latitudinal-and-seasonal dependent WACCM climatology	ECMWF[3]
Calibration factor	0.830	1.0 (Wunch et al., 2011)	0.88	None	None
Number of degrees of freedom			2.8	4-5	

References

Allan, R.P.: The Role of Water Vapour in Earth's Energy Flows. Surveys in Geophysics, 33, 557–564, https://doi.org/10.1007/s10712-011-9157-8, 2012.

Alraddawi, D., Sarkissian, A., Keckhut, P., Bock, O., Noël, S., Bekki, S., Irbah, A., Meftah, M., and Claud, C.: Comparison of total water vapour content in the Arctic derived from GNSS, AIRS, MODIS and SCIAMACHY, Atmos. Meas. Tech., 11, 2949–2965, https://doi.org/10.5194/amt-11-2949-2018, 2018.

Blumenstock, T., Kopp, G., Hase, F., Hochschild, G., Mikuteit, S., Raffalski, U., and Ruhnke, R.: Observation of unusual chlorine activation by ground-based infrared and microwave spectroscopy in the late Arctic winter 2000/01, Atmos. Chem. Phys., 6, 897–905, https://doi.org/10.5194/acp-6-897-2006, 2006.

Barthlott, S., Schneider, M., Hase, F., Blumenstock, T., Kiel, M., Dubravica, D., García, O. E., Sepúlveda, E., Mengistu Tsidu, G., Takele Kenea, S., Grutter, M., Plaza-Medina, E. F., Stremme, W., Strong, K., Weaver, D., Palm, M., Warneke, T., Notholt, J., Mahieu, E., Servais, C., Jones, N., Griffith, D. W. T., Smale, D., and Robinson, J.: Tropospheric water vapour isotopologue data ($H_2{}^{16}O$, $H_2{}^{18}O$, and $HD^{16}O$) as obtained from NDACC/FTIR solar absorption spectra, Earth Syst. Sci. Data, 9, 15–29, https://doi.org/10.5194/essd-9-15-2017, 2017.

Borger, C., Schneider, M., Ertl, B., Hase, F., García, O. E., Sommer, M., Höpfner, M., Tjemkes, S. A., and Calbet, X.: Evaluation of MUSICA IASI tropospheric water vapour profiles using theoretical error assessments and comparisons to GRUAN Vaisala RS92 measurements, Atmos. Meas. Tech., 11, 4981–5006, https://doi.org/10.5194/amt-11-4981-2018, 2018.

Buehler, S. A., Östman, S., Melsheimer, C., Holl, G., Eliasson, S., John, V. O., Blumenstock, T., Hase, F., Elgered, G., Raffalski, U., Nasuno, T., Satoh, M., Milz, M., and Mendrok, J.: A multi-instrument comparison of integrated water vapour measurements at a high latitude site, Atmos. Chem. Phys., 12, 10925–10943, https://doi.org/10.5194/acp-12-10925-2012, 2012.

Butz, A., Dinger, A. S., Bobrowski, N., Kostinek, J., Fieber, L., Fischerkeller, C., Giuffrida, G. B., Hase, F., Klappenbach, F., Kuhn, J., Lübcke, P., Tirpitz, L., and Tu, Q.: Remote sensing of volcanic CO2, HF, HCl, SO2, and BrO in the downwind plume of Mt. Etna, Atmos. Meas. Tech., 10, 1–14, https://doi.org/10.5194/amt-10-1-2017, 2017.

Clerbaux, C., Boynard, A., Clarisse, L., George, M., Hadji-Lazaro, J., Herbin, H., Hurtmans, D., Pommier, M., Razavi, A., Turquety, S., Wespes, C., and Coheur, P.-F.: Monitoring of atmospheric composition using the thermal infrared IASI/MetOp sounder, Atmospheric Chemistry and Physics, 9, 6041–6054, doi:10.5194/acp-9-6041-2009, 2009.

Chen, J., Viatte, C., Hedelius, J. K., Jones, T., Franklin, J. E., Parker, H., Gottlieb, E. W., Wennberg, P. O., Dubey, M. K., and Wofsy, S. C.: Differential column measurements using compact solar-tracking spectrometers, Atmos. Chem. Phys., 16, 8479–8498, https://doi.org/10.5194/acp-16-8479-2016, 2016.

Chazette, P., Marnas, F., Totems, J., and Shang, X.: Comparison of IASI water vapor retrieval with H2O-Raman lidar in the framework of the Mediterranean HyMeX and ChArMEx programs, Atmos. Chem. Phys., 14, 9583–9596, https://doi.org/10.5194/acp-14-9583-2014, 2014.

De Mazière, M., Thompson, A. M., Kurylo, M. J., Wild, J. D., Bernhard, G., Blumenstock, T., Braathen, G. O., Hannigan, J. W., Lambert, J.-C., Leblanc, T., McGee, T. J., Nedoluha, G., Petropavlovskikh, I., Seckmeyer, G., Simon, P. C., Steinbrecht, W., and Strahan, S. E.: The Network for the Detection of Atmospheric Composition Change (NDACC): history, status and perspectives, Atmos. Chem. Phys., 18, 4935–4964, https://doi.org/10.5194/acp-18-4935-2018, 2018.

Delamere, J. S., Clough, S. A., Payne, V. H., Mlawer, E. J., Turner, D. D. and Gamache, R. R.: A far-infrared radiative closure study in the Arctic: application to water vapor. J. Geophys. Res. 115, D17106. doi:10.1029/2009JD012968, 2010.

Dirksen, R. J., Sommer, M., Immler, F. J., Hurst, D. F., Kivi, R., and Vömel, H.: Reference quality upper-air measurements: GRUAN data processing for the Vaisala RS92 radiosonde, Atmos. Meas. Tech., 7, 4463–4490, https://doi.org/10.5194/amt-7-4463-2014, 2014.

Dupuy, E., Morino, I., Deutscher, N.M., Yoshida, Y., Uchino, O., Connor, B.J., De Mazière, M., Griffith, D.W.T., Hase, F., Heikkinen, P., Hillyard, P.W., Iraci, L.T., Kawakami, S., Kivi, R., Matsunaga, T., Notholt, J., Petri, C., Podolske, J.R., Pollard, D.F., Rettinger, M., Roehl, C.M., Sherlock, V., Sussmann, R., Toon, G.C., Velazco, V.A., Warneke, T., Wennberg, P.O., Wunch, D., Yokota, T.: Comparison of XH2O Retrieved from GOSAT Short-Wavelength Infrared Spectra with Observations from the TCCON Network. Remote Sensing, 8, 414, 2016.

Frey, M., Hase, F., Blumenstock, T., Groß, J., Kiel, M., Mengistu Tsidu, G., Schäfer, K., Sha, M. K., and Orphal, J.: Calibration and instrumental line shape characterization of a set of portable FTIR spectrometers for detecting greenhouse gas emissions, Atmos. Meas. Tech., 8, 3047–3057, https://doi.org/10.5194/amt-8-3047-2015, 2015.

Frey, M., Sha, M. K., Hase, F., Kiel, M., Blumenstock, T., Harig, R., Surawicz, G., Deutscher, N. M., Shiomi, K., Franklin, J. E., Bösch, H., Chen, J., Grutter, M., Ohyama, H., Sun, Y., Butz, A., Mengistu Tsidu, G., Ene, D., Wunch, D., Cao, Z., Garcia, O., Ramonet, M., Vogel, F., and Orphal, J.: Building the COllaborative Carbon Column Observing Network (COCCON): long-term stability and ensemble performance of the EM27/SUN Fourier transform spectrometer, Atmos. Meas. Tech., 12, 1513–1530, https://doi.org/10.5194/amt-12-1513-2019, 2019.

Gisi, M., Hase, F., Dohe, S., Blumenstock, T., Simon, A., and Keens, A.: XCO2-measurements with a tabletop FTS using solar absorption spectroscopy, Atmos. Meas. Tech., 5, 2969–2980, https://doi.org/10.5194/amt-5-2969-2012, 2012.

Jacobs, N., Simpson, W. R., Wunch, D., O'Dell, C. W., Osterman, G. B., Hase, F., Blumenstock, T., Tu, Q., Frey, M., Dubey, M. K., Parker, H. A., Kivi, R., and Heikkinen, P.: Quality controls, bias, and seasonality of CO2 columns in the boreal forest with Orbiting Carbon Observatory-2, Total Carbon Column Observing Network, and EM27/SUN measurements, Atmos. Meas. Tech., 13, 5033–5063, https://doi.org/10.5194/amt-13-5033-2020, 2020.

Hase, F., Frey, M., Blumenstock, T., Groß, J., Kiel, M., Kohlhepp, R., Mengistu Tsidu, G., Schäfer, K., Sha, M. K., and Orphal, J.: Application of portable FTIR spectrometers for detecting greenhouse gas emissions of the major city Berlin, Atmos. Meas. Tech., 8, 3059–3068, https://doi.org/10.5194/amt-8-3059-2015, 2015.

Hase, F., Hanningan, J. W., Coffey, M. T., Goldman, A., Höpfner, M., Jones, N. B., Rinsland, C. P., and Wood, S. W.: Intercomparison of retrieval codes used for the analysis of highresolution ground-based FTIR measurements, J. Quant. Spectrosc. Ra., 87, 25–52, 2004.

Hase, F., Frey, M., Kiel, M., Blumenstock, T., Harig, R., Keens, A., and Orphal, J.: Addition of a channel for XCO observations to a portable FTIR spectrometer for greenhouse gas measurements, Atmos. Meas. Tech., 9, 2303–2313, https://doi.org/10.5194/amt9-2303-2016, 2016.

Hedelius, J. K., Viatte, C., Wunch, D., Roehl, C. M., Toon, G. C., Chen, J., Jones, T., Wofsy, S. C., Franklin, J. E., Parker, H., Dubey, M. K., and Wennberg, P. O.: Assessment of errors and biases in retrievals of XCO2, XCH4, XCO, and XN2O from a 0.5 cm–1 resolution solar-viewing spectrometer, Atmos. Meas. Tech., 9, 3527–3546, https://doi.org/10.5194/amt-9-3527-2016, 2016.

Hu, H., Landgraf, J., Detmers, R., Borsdorff, T., Aan de Brugh, J., Aben, I., Butz, A. and Hasekamp O.: Toward global mapping of methane with TROPOMI: First results and intersatellite comparison to GOSAT. Geophysical Research Letters, 45, 3682– 3689. https://doi.org/10.1002/2018GL077259, 2018.

Hyland, R. W. and Wexler, A.: Formulations for the Thermodynamic Properties of the saturated Phases of H2O from 173.15K to 473.15K, ASHRAE Trans, 89(2A), 500-519, 1983.

Isaac, V., and van Wijngaarden, W. A. Surface Water Vapor Pressure and Temperature Trends in North America during 1948–2010. J. Climate, 25, 3599–3609, https://doi.org/10.1175/JCLI-D-11-00003.1, 2012.

Kiehl, J. T. and K. E. Trenberth: Earth's Annual Global Mean Energy Budget, Bulletin of the American Meteorological Society, 78(2): 197-208, 1997.

Klappenbach, F., Bertleff, M., Kostinek, J., Hase, F., Blumenstock, T., Agusti-Panareda, A., Razinger, M., and Butz, A.: Accurate mobile remote sensing of XCO2 and XCH4 latitudinal transects from aboard a research vessel, Atmos. Meas. Tech., 8, 5023–5038, doi:10.5194/amt-8-5023-2015, 2015.

Kivi, R. and Heikkinen, P.: Fourier transform spectrometer measurements of column CO2 at Sodankylä, Finland, Geosci. Instrum. Method. Data Syst., 5, 271–279, https://doi.org/10.5194/gi-5-271-2016, 2016.

Kivi, R., Heikkinen, P. and Kyrö, E.: TCCON Data from Sodankylä, Finland, Release GGG2014R0, TCCON Data Archive, Hosted by CaltechDATA, California Institute of Technology: Pasadena, CA, USA, doi:10.14291/tccon.ggg2014.sodankyla01.R0/1149280, 2017.

Kurylo, M. and Zander, R.: The NDSC – Its status after 10 years of operation, Proceedings of the XIX Quadrennial Ozone Symposium, Hokkaido University, Sapporo, Japan, 167–168, 2000.

Loew, A., Bell, W., Brocca, L., Bulgin, C. E., Burdanowitz, J, Calbet, X., Donner, R. V., Ghent, D, Gruber, A., Kaminski, T., Kinzel, J., Klepp, C., Lambert, J., Schäpman-Strub, G., Schröder, M., Verhoelst, T.: Validation practices for satellite-based Earth observation data across communities. Reviews of Geophysics, Vol. 55, 779–817, doi:10.1002/2017RG000562, 2017.

Mlawer, E. J., Payne, V. H., Moncet, J.-L., Delamere, J. S., Alvarado, M. J. and Tobin, D. C.: Development and recent evaluation of the MT_CKD model of continuum absorption. Phil. Trans. R. Soc. A.3702520–2556, http://doi.org/10.1098/rsta.2011.0295, 2012.

Madonna, F., Kivi, R., Dupont, J.-C., Ingleby, B., Fujiwara, M., Romanens, G., Hernandez, M., Calbet, X., Rosoldi, M., Giunta, A., Karppinen, T., Iwabuchi, M., Hoshino, S., von Rohden, C., and Thorne, P. W.: Use of automatic radiosonde launchers to measure temperature and humidity profiles from the GRUAN perspective, Atmos. Meas. Tech., 13, 3621–3649, https://doi.org/10.5194/amt-13-3621-2020, 2020.

Pałm, M., Melsheimer, C., Noël, S., Heise, S., Notholt, J., Burrows, J., and Schrems, O.: Integrated water vapor above Ny Ålesund, Spitsbergen: a multi-sensor intercomparison, Atmos. Chem. Phys., 10, 1215–1226, https://doi.org/10.5194/acp-10-1215-2010, 2010.

Payne, V. H., Mlawer, E. J., Cady-Pereira, K. E. and Moncet, J.-L.: Water Vapor Continuum Absorption in the Microwave. Geoscience and Remote Sensing, IEEE Transactions on. 49. 2194 - 2208. 10.1109/TGRS.2010.2091416, 2011.

Rodgers, C. D. and Connor, B. J.: Intercomparison of Remote Sounding Instruments, J. Geophys. Res., 108, doi:10.1029/2002JD002299, 2003.

Scheepmaker, R. A., aan de Brugh, J., Hu, H., Borsdorff, T., Frankenberg, C., Risi, C., Hasekamp, O., Aben, I., and Landgraf, J.: HDO and H2O total column retrievals from TROPOMI shortwave infrared measurements, Atmos. Meas. Tech., 9, 3921–3937, https://doi.org/10.5194/amt-9-3921-2016, 2016.

Schneider, A., Borsdorff, T., aan de Brugh, J., Aemisegger, F., Feist, D. G., Kivi, R., Hase, F., Schneider, M., and Landgraf, J.: First data set of H2O/HDO columns from the Tropospheric Monitoring Instrument (TROPOMI), Atmos. Meas. Tech., 13, 85–100, https://doi.org/10.5194/amt-13-85-2020, 2020.

Schneider, M., Hase, F., and Blumenstock, T.: Water vapour profiles by ground-based FTIR spectroscopy: study for an optimised retrieval and its validation, Atmos. Chem. Phys., 6, 811–830, https://doi.org/10.5194/acp-6-811-2006, 2006.

Schneider, M. and Hase, F.: Ground-based FTIR water vapour profile analyses, Atmos. Meas. Tech., 2, 609–619, https://doi.org/10.5194/amt-2-609-2009, 2009.

Schneider, M., Romero, P. M., Hase, F., Blumenstock, T., Cuevas, E., and Ramos, R.: Continuous quality assessment of atmospheric water vapour measurement techniques: FTIR, Cimel, MFRSR, GPS, and Vaisala RS92, Atmos. Meas. Tech., 3, 323–338, doi:10.5194/amt-3-323-2010, 2010a.

Schneider, M., Yoshimura, K., Hase, F., and Blumenstock, T.: The ground-based FTIR network's potential for investigating the atmospheric water cycle, Atmos. Chem. Phys., 10, 3427–3442, doi:10.5194/acp-10-3427-2010, 2010b.

Schneider, M. and Hase, F.: Optimal estimation of tropospheric H2O and δD with IASI/METOP, Atmos. Chem. Phys., 11, 11207–11220, https://doi.org/10.5194/acp-11-11207-2011, 2011.

Schneider, M., Barthlott, S., Hase, F., González, Y., Yoshimura, K., García, O. E., Sepúlveda, E., Gomez-Pelaez, A., Gisi, M., Kohlhepp, R., Dohe, S., Blumenstock, T., Wiegele, A., Christner, E., Strong, K., Weaver, D., Palm, M., Deutscher, N. M., Warneke, T., Notholt, J., Lejeune, B., Demoulin, P., Jones, N., Griffith, D. W. T., Smale, D., and Robinson, J.: Ground-based remote sensing of tropospheric water vapour isotopologues within the project MUSICA, Atmos. Meas. Tech., 5, 3007–3027, https://doi.org/10.5194/amt-5-3007-2012, 2012.

Schneider, M., Wiegele, A., Barthlott, S., González, Y., Christner, E., Dyroff, C., García, O. E., Hase, F., Blumenstock, T., Sepúlveda, E., Mengistu Tsidu, G., Takele Kenea, S., Rodríguez, S., and Andrey, J.: Accomplishments of the MUSICA project to provide accurate, long-term, global and high-resolution observations of tropospheric {H2O, δD} pairs – a review, Atmospheric Measurement Techniques, 9, 2845–2875, https://doi.org/10.5194/amt-9-2845-2016, 2016.

Sha, M. K., De Mazière, M., Notholt, J., Blumenstock, T., Chen, H., Dehn, A., Griffith, D. W. T., Hase, F., Heikkinen, P., Hermans, C., Hoffmann, A., Huebner, M., Jones, N., Kivi, R., Langerock, B., Petri, C., Scolas, F., Tu, Q., and Weidmann, D.: Intercomparison of low and high resolution infrared spectrometers for ground-based solar remote sensing measurements of total column concentrations of CO2, CH4 and CO, Atmos. Meas. Tech. Discuss., https://doi.org/10.5194/amt-2019-371, in review, 2019.

Soden, B. J., Wetherald, R. T., Stenchikov, G. L. and Robock, A.: Global cooling after the eruption of Mount Pinatubo: A test of climate feedback by water vapor, Science, 296, 727–730, doi:10.1126/science.296.5568.727, 2002.

Trenberth, K. E.: Atmospheric moisture residence times and cycling: Implications for rainfall rates and climate change. Climatic Change, 39, 667–694, https://doi.org/10.1023/A:1005319109110, 1998.

Trieu, T.T.N., Morino, I., Ohyama, H., Uchino, O., Sussmann, R., Warneke, T., Petri, C., Kivi, R., Hase, F., Pollard, D.F., Deutscher, N.M., Velazco, V.A., Iraci, L.T., Podolske, J.R., Dubey, M.K.: Evaluation of Bias Correction Methods for GOSAT SWIR XH2O Using TCCON data, Remote Sensing, 11, 290, doi:10.3390/rs11030290, 2019.

Tu, Q., Hase, F., Blumenstock, T., Kivi, R., Heikkinen, P., Sha, M. K., Raffalski, U., Landgraf, J., Lorente, A., Borsdorff, T., and Chen, H.: Atmospheric CO2 and CH4 abundances on regional scales in boreal areas using CAMS reanalysis, COCCON spectrometers and Sentinel-5 Precursor satellite observations, Atmos. Meas. Tech. Discuss., https://doi.org/10.5194/amt-2020-19, in review, 2020.

Veefkind, J., Aben, I., McMullan, K., örster, H., de Vries, J., Otter, G., Claas, J., Eskes, H., de Haan, J., Kleipool, Q., vanWeele, M., Hasekamp, O., Hoogeveen, R., Landgraf, J., Snel, R., Tol, P., Ingmann, P., P., V., Kruizinga, P., Vink, R., Visser, H., and Levelt, P.: TROPOMI on the ESA Sentinel-5 Precursor: A GMES mission for global observations of the atmospheric composition for climate, air quality and ozone layer applications, Remote Sens. Environ., 120, 70–83, doi:10.1016/j.rse.2011.09.027, 2012.

Vogel, F., Frey, M., Staufer, J., Hase, F., Broquet, G., Xueref-Remy, I., Chevallier, F., Ciais, P., Sha, M.K., Chelin, P., Jeseck, P., Janssen, C., Te, Y., Groß, J., Blumenstock, T., Tu, Q., Orphal, J.: XCO2 in an emission hot- spot region: the COCCON Paris campaign 2015, Atmospheric Chemistry and Physics, doi: 10.5194/acp-19-3271-2019, 2019.

Vogelmann, H., Sussmann, R., Trickl, T., and Reichert, A.: Spatiotemporal variability of water vapor investigated using lidar and FTIR vertical soundings above the Zugspitze, Atmospheric Chemistry and Physics, 15, 3135–3148, https://doi.org/10.5194/acp-15-3135-2015, 2015.

Wunch, D., Toon, G. C., Blavier, J.-F. L., Washenfelder, R. A., Notholt, J., Connor, B. J., Griffith, D. W. T., Sherlock, V., and Wennberg, P. O.: The total carbon column observing network, Philos. T. R. Soc. A, 369, 2087–2112, doi:10.1098/rsta.2010.0240, 2011.

Wunch, D., Toon, G. C., Sherlock, V., Deutscher, N. M., Liu,C., Feist, D. G., and Wennberg, P. O.: The Total CarbonColumn Observing Network's GGG2014 Data Version, Tech.rep., California Institute of Technology, Carbon Dioxide In-formation Analysis Center, Oak Ridge National Laboratory,Oak Ridge, Tennessee, USA, https://doi.org/10.14291/tccon.ggg2014.documentation.R0/1221662, 2015.

Wunch, D., Wennberg, P. O., Osterman, G., Fisher, B., Naylor, B., Roehl, C. M., O'Dell, C., Mandrake, L., Viatte, C., Kiel, M., Griffith, D. W. T., Deutscher, N. M., Velazco, V. A., Notholt, J., Warneke, T., Petri, C., De Maziere, M., Sha, M. K., Sussmann, R., Rettinger, M., Pollard, D., Robinson, J., Morino, I., Uchino, O., Hase, F., Blumenstock, T., Feist, D. G., Arnold, S. G., Strong, K., Mendonca, J., Kivi, R., Heikkinen, P., Iraci, L., Podolske, J., Hillyard, P. W., Kawakami, S., Dubey, M. K., Parker, H. A., Sepulveda, E., García, O. E., Te, Y., Jeseck, P., Gunson, M. R., Crisp, D., and Eldering, A.: Comparisons of the Orbiting Carbon Observatory-2 (OCO-2) XCO2 measurements with TCCON, Atmos. Meas. Tech., 10, 2209–2238, https://doi.org/10.5194/amt-10-2209-2017, 2017.

Wypych, A., Bochenek, B. and Różycki, M.: Atmospheric Moisture Content over Europe and the Northern Atlantic. Atmosphere, 9, 18, https://doi.org/10.3390/atmos9010018, 2018.